AN ABSTRACT OF THE THESIS OF

Bilqees Azim for the degree of Master of Science in Nuclear Engineering presented on July 12, 1988.

Title: Elemental Analysis of Zircon Samples from Pacific Northwest Beaches by INAA

Abstract approved: Redacted for Privacy

Stephen E. Binney

Fifteen sand samples from beaches along the Pacific North were analyzed for their elemental content by the method of instrumental neutron activation analysis (INAA). A separation technique was employed to separate the zircon (a heavy non-magnetic mineral with a specific gravity of 4.67) from the rest of the sample. This technique worked fairly well for most of the samples. The zircon content of the heavy non-magnetic samples was in the range of 58 - 95%, except for two northern California beaches which contained appreciable quantities of rutile. The hafnium content of the heavy non-magnetic sample was fairly constant. The

rare earth pattern in the heavy non-magnetic samples was similar to that observed in geological samples.

At present, the Oregon beaches are not economically minable for zircon.

ELEMENTAL ANALYSIS OF ZIRCON SAMPLES FROM PACIFIC NORTHWEST BEACHES BY INAA

by

Bilqees Azim

A THESIS

submitted to

Oregon State University

in partial fulfillment of
the requirements for the
degree of

Master of Science

Completed July 12, 1988

Commencement June 1989

APPROVED:

Redacted for Privacy

Professor of Nuclear Engineering

Redacted for Privacy

Head of department of Nuclear Engineering

Redacted for Privacy

Dean of Graduate School

Date Thesis is presented July 12, 1988

ACKNOWLEDGEMENT

I would like to express sincere thanks to my major professor, Dr. Stephen E. Binney, for his advice and recommendations during the course of my project work. His help is deeply appreciated. Working with him was a great experience and will always be remembered.

I am very thankful to my committee, Dr Roman A. Schmitt, Dr. Andrew C.Klein, and Dr. Jonathan D. Istok. I would also like to thank Dr. Curt D. Peterson and Margaret Mumford of College of Oceanography, for their advice in preparing samples, and Mike Conrady of Radiation Center, for his help with the data reduction programs.

A special thanks to my fiancé, Saleem, for his encouragement and understanding.

I would also like to thank my friends, Jeff Samuals, Steve Gedeon, and Ajay Anand for their help with the word processor, proof reading the thesis draft, and their moral support.

I dedicate this thesis to my parents, Ayesha and Azim, who always encouraged and supported me from so far away.

TABLE OF CONTENTS

LIST OF FIGURES

LIST OF TABLES

ELEMENTAL ANALYSIS OF ZIRCON SAMPLES FROM PACIFIC NORTHWEST BEACHES BY INAA

1. INTRODUCTION

The ocean beaches, continental shelves and seabed can be a vast source of minerals, causing marine geology to become increasingly important every day because of its potential. Knowledge about marine geology has been accumulating in recent years. The data collected have led scientists to reformulate theories about mineral deposits and have enabled them to make

better predictions about new deposits. Knowledge of mineral deposits on land provides clues about the nature and possible location of offshore minerals. For example, beach sands containing heavy minerals such as chromite or ilmenite may help identify likely locations and compositions of similar deposits located in the nearshore areas [1].

The major elements for which the beach and shelf samples are being investigated are elements which are relatively scarce, but have a technological importance, such as Ti, Cr, V, Zr and Hf. Each of these elements has its own significance in the aviation, electronics or nuclear industry. At present the U.S. imports minerals containing Cr and Ti from countries which are not politically stable, and hence a long term supply of these minerals may not be guaranteed.

One of the ultimate goals of all the research being carried out in this field (of which this project is a part) is to find a correlation between the location and the concentration of particular elements of interest which would lead to an accurate predictive model for the sources of these minerals [2].

At present, seabed mining is not an economically viable venture, but depletion of land resources would eventually make the prospect of seabed mining economically feasible. Throughout the world, rapidly

growing industrialization is causing an ever-increasing demand for raw materials. For this reason, the seabed is gradually drawing increased attention as a source of some of the elements that are in short supply [3]. Therefore the prospect of seabed mining is being treated as a long term project and the vast mineral resources are considered to be important assets for the future. Consequently, a great deal of effort is being made to explore the seabed for important minerals and to develop technology according to the requirements of seabed mining.

Several techniques, including neutron activation analysis, have been developed recently to explore the seabed for mineral deposits [4, 5]. Preliminary research indicates that the method of neutron activation analysis can play an important part in "in-situ" evaluation and analysis of seabed samples [6, 7, 8].

In this project the sample analysis was carried out with an emphasis on the elemental content of the mineral zircon. Zirconium, the major component of zircon, is an important material in the nuclear industry. It is used as a nuclear reactor fuel cladding material due to its extremely low thermal neutron absorption cross section and its corrosion resistance properties [9].

Zirconium is distributed widely in the earth's crust, ranking eleventh in relative abundance of

elements in igneous rocks. It is more abundant than Cu, Pb, Zn and Ni, and has an abundance of 220 g per ton (243 g/tonne). Hafnium, which is geochemically associated with Zr, has an abundance of 4.5 g per ton (5.0 g/tonne) and is more plentiful than Hg, Sb, and Bi [10].

There are at least 37 zirconium-bearing minerals found in nature; about 21 of these contain zircon as an essential constituent. Therefore zircon is the chief ore of Zr and is a common accessory mineral in siliceous igneous rocks, crystalline limestones, sedimentary rocks derived from schists and gneisses, and in beach and river placer deposits. However zircon is found only rarely in the hard rock deposits in minable concentrations. Hence the principal world reserves of zircon are in alluvial and beach sand deposits in which the zircon is associated with one and more of the heavy minerals such as magnetite, ilmenite, rutile, monazite, and many others [11].

Zirconium is also present in the minerals zirfesite($\sim ZrO_2Fe_2O_3SiO_2.nH_2O$), zirkelite ($\{(Ca,Th,La)Zr(Ti,Nb,Fe)_2O_7\}$), and zirsinilite ($\{Na(Ca,Mn,Fe)Zr(SiO_3)_6\}$) [12]. However these are the less commonly occurring minerals of zirconium and not as economically minable as zircon.

Zirconium minerals, mainly zircon, have many uses

in which the presence of Hf is immaterial. For example, zircon is used as a refractory, and, when cut and polished, the colorless varieties provide gemstones [13]. In nuclear energy applications, however, the two metals must be separated because they exhibit opposite properties in the presence of thermal neutrons.

In an earlier work by Dr. G. W. Gleeson it was found that in the sand samples from Oregon, the concentration of zircon was as much as 10% [14]; these sands also had considerable concentrations of Ti, Cr, Fe and Hf (the latter always found with Zr) in the form of oxides. Comparative data were collected by analyzing samples from different locations, and a relative abundance of the abovementioned minerals was determined.

In this project fifteen samples from the beaches along the northern Pacific coast of the United States were analyzed primarily for zirconium and also for other major elements (present in the percent range), minor elements (present in fractions of a percent) and trace elements (present in parts per million). These samples were obtained from the Oregon State University (OSU) College of Oceanography.

Zirconium is present in these beach sands as zircon, which is $ZrSiO_4$. Zircon is a heavy mineral of specific gravity 4.67; therefore the samples were

subjected to separation techniques designed to isolate zircon from rest of the sample. Table A-1 in Appendix A shows some of the geological properties of zircon, and Table A-2 shows some of the chemical properties of Zr.

The method of analysis which was chosen for this project was instrumental neutron activation analysis (INAA), which has a wide application in sample analyses of all kinds. Sequential neutron activation analyses can measure up to 37 major, minor and trace elements in a sample [15].

The results presented are based on an analysis of all the data collected for the samples.

2. SAMPLE DESCRIPTION AND PREPARATION

2.1 SAMPLE DESCRIPTION

2.1.1 Location

The samples were collected from the beaches along the Pacific coast shoreline. The beaches were located in Northern California, along the Oregon coastline, and in the state of Washington. Table 1 shows the state and the latitude location of these samples. The samples were chosen on the basis that they span a wide geographic range along the Pacific coast. Fig. 1 shows the location of the beaches from which the samples were collected. These samples as collected are termed the bulk samples.

2.1.2 General composition

The bulk samples consisted of three classes of minerals [16]:

a. Light: quartz, silica, feldspar
b. Heavy (Magnetic): chromite, ilmenite, garnet, epidote, zoisite
c. Heavy (Non-magnetic): zircon, rutile

TABLE 1

Location of the bulk samples

Sample	Latitude, °N (south to north)	State
Moonstone	41.04	California
N. Fern Canyon	41.47	California
Crescent City	41.73	California
Hunters Cove	42.32	Oregon
Nesika	42.50	Oregon
Port Orford	42.73	Oregon
Cape Blanco	42.84	Oregon
Sacci	43.21	Oregon
Heceta	44.03	Oregon
Agate	44.67	Oregon
Roads End	45.01	Oregon
Meriweather	45.31	Oregon
Manzanita	45.72	Oregon
Ocean Beach	46.22	Oregon
Beach # 3	47.65	Washington

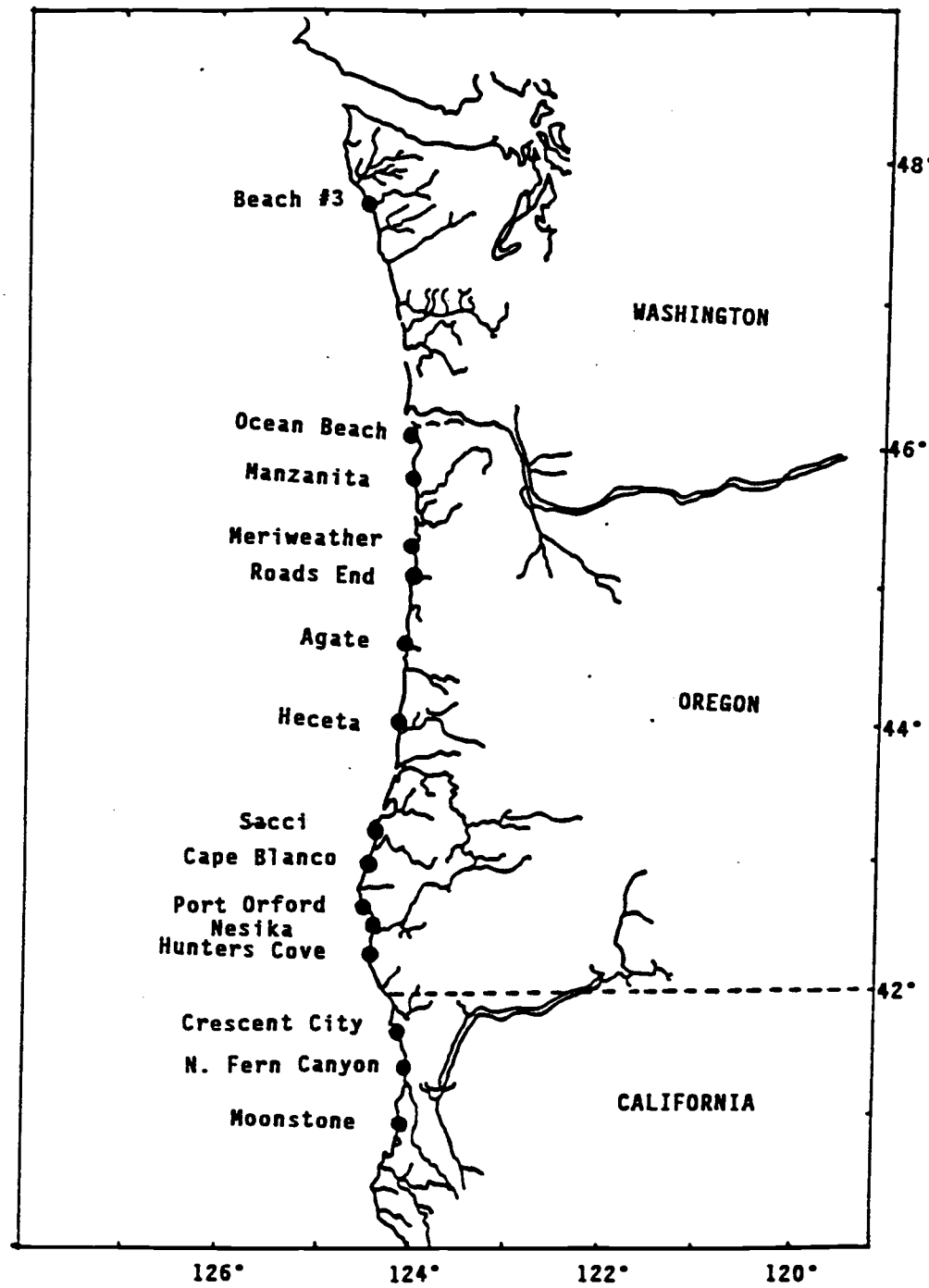

Fig. 1. Locations of the bulk samples

Zircon resided in the heavy non-magnetic part of the bulk samples, its specific gravity being 4.67. Although the focus of this effort was mainly on Zr and its "twin" element Hf, the possibility of finding other trace elements was not ruled out. Also the efficiency of the separation procedures was not previously established; therefore it was reasonable to assume that other minerals would be present in the separated samples to some extent.

2.2 SAMPLE SEPARATION

Sample preparation formed an important part of this project because of the intricate procedures involved. These procedures were termed as microtechniques and consisted of separation of the desired part of the sample from other parts which were not deemed of interest for analysis.

The sample separation techniques followed the order of (1) separation of heavy minerals from light ones at a specific gravity of 3.0, (2) separation of the heavy minerals into magnetic and non-magnetic minerals, and (3) a separation of the non-magnetic minerals at a specific gravity of 4.2. These techniques involved the use of sodium polytungstate which is a dense solution with a specific gravity of 3.0, a hand magnet and a

Frantz magnetic separator, and tungsten carbide (WC) which has a density of 15.6 g/cm^3. In the final step of separation, tungsten carbide was added to sodium polytungstate to make a colloidal solution of specific gravity 4.2.

In the procedures for sample separation, extra care was taken so as not to introduce any contamination in the samples. In different steps where the samples were processed one after the other, extreme caution was required so that traces of one sample were not mixed with another. Starting from the bulk sample, the separation followed a stepwise procedure, which is the essence of microtechniques. The main steps of the separation scheme are shown in Fig. 2. This separation scheme was followed for only that part of the sample which was pertinent to this project.

2.2.1 Sieving.

Sieving was carried out mainly to separate out rock fragments and other larger particles of silica and quartz which were not of interest for this analysis. In this step, a stack of brass sieves of mesh size 1 mm to 170 microns was placed in ascending order, with the smallest mesh on the bottom. The sieves were made of steel and there were eight sieves in total. About 100 g of the bulk sample was placed in the top sieve. This

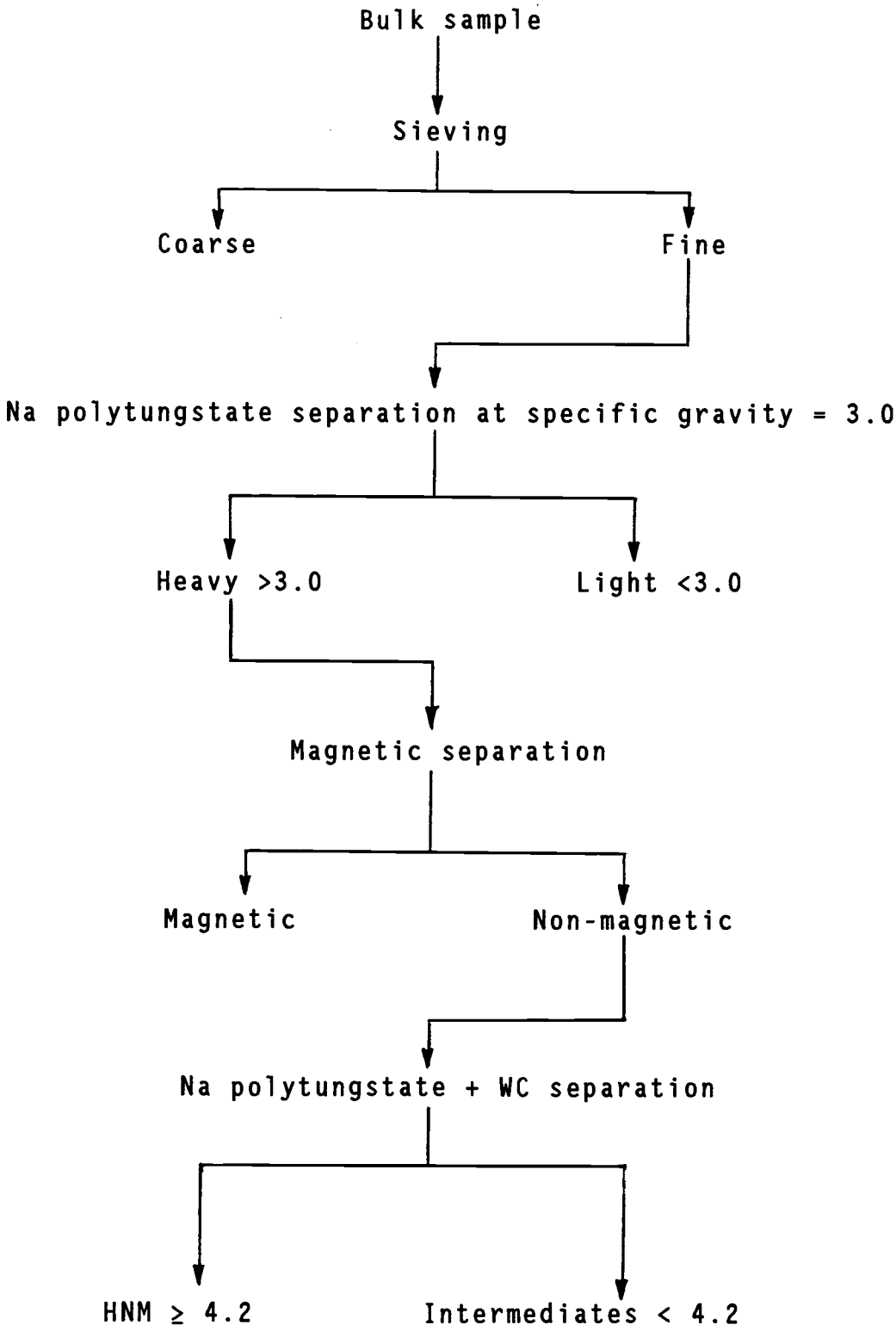

Fig. 2. Sample separation scheme

stack of brass sieves was secured on top of a vibrator with rubber tubing attached to the vibrator. The vibrator was switched on and allowed to work for fifteen minutes. All the particles from 210 microns down were taken as fine grains consisting of relatively heavy particles. Both the coarse and the fine grains were weighed and the weights were recorded. In this step the samples were not washed.

2.2.2 Sodium polytungstate separation (separation at 3.0 specific gravity).

In this step the aim was to achieve a separation of the fine fraction at a specific gravity of 3.0 to remove the light minerals such as quartz and feldspar in the sample. This step also reduced the sample mass, which speeded up the later separation steps.

For this separation a sodium polytungstate solution, which had a specific gravity of 3.0, was used. To begin, the sodium polytungstate solution was poured into a beaker. For every 10 g of a particular sample, 20 ml of sodium polytungstate was required. The sample was stirred into this solution and allowed to settle for about 12 hours. The grains of greater than 3.0 specific gravity settled down in the bottom, while the lighter grains floated on the top.

Once the separation had occurred, liquid nitrogen

was used to isolate the light and heavy minerals. Liquid nitrogen was poured into a large beaker and the smaller beaker containing the separated portions of the sample in the sodium polytungstate was lowered carefully into the liquid nitrogen without disturbing the contents. The bottom part of the solution, where the heavier particles were settled, was frozen completely. Appropriate quantities of nitrogen were added to ensure this. The lighter particles floating at the top were then washed off with distilled water into a funnel lined with filter paper. The heavier particles thawed after several minutes and were washed off into a different funnel. The samples in their respective funnels were thoroughly rinsed to wash off the sodium polytungstate, since both sodium and tungsten are contaminants for later sample analysis. Another reason for thorough rinsing was to prevent the samples from drying out in lumps, which would require a rewashing.

After washing the samples, the light and the heavy parts of the sample were folded in their respective filter papers and left in an oven to dry. The oven was operated at a temperature of 80 °C and the samples were left for a period of 12 hours (or overnight). The "lights" (specific gravity <3.0), and the "heavies" (specific gravity >3.0) were weighed after drying, and the weights were recorded.

2.2.3 Magnetic separation.

The main object of this separation process was to get the fraction of the sample which was non-magnetic or nearly so. Zircon is a non-magnetic substance, and the magnetic minerals, such as magnetite, chromite, ilmenite and garnet, were removed in this step. All of these minerals, including zircon, are heavier than a specific gravity of 4.0, but the zircon remains in the residual sample because of its non-magnetic character.

A hand magnet was used first for the removal of strongly magnetic substances such as magnetite and pyroxenes. This method was efficient and it averted clogging in the Frantz separator.

In the Frantz separator, which is an isodynamic magnetic separator, a series of current settings were required to separate out the magnetic minerals. Initially the current was set at 0.4 A and the tilt angle was set at 20°. The sample was run through the separator once and then the non-magnetic portion was run through at least three times again to remove as much of the magnetic particles as possible. These settings removed ilmenite, chromite and garnet. Next the current was increased to 0.8 A to remove less magnetic minerals such as epidote, chlorite and dark tourmaline. At the current setting of 1.2 A, minerals of even less magnetic susceptibility, such as zoisite and light tourmaline

were removed. The tilt angle was then changed to 5°, keeping the current setting at 1.2 A, to extract minerals such as sphene and monazite. At each setting the portion of the sample retained as non-magnetic was run through the Frantz separator to clean the sample of magnetic minerals as much as possible. The magnetic and the non-magnetic portions were weighed, and the masses were registered.

2.2.4 Tungsten carbide-sodium polytungstate separation.

After the magnetic separation, the samples consisted of minerals which had a specific gravity of at least 3.0 and were non-magnetic. Therefore a further separation was required to obtain a sample which would consist largely of zircon. In this step a colloidal mixture of tungsten carbide and sodium polytungstate was prepared which had a specific gravity of 4.2.

The tungsten carbide-sodium polytungstate mixture was prepared by pouring about 10 ml of sodium polytungstate into a 100 ml cylinder which had previously been weighed. Tungsten carbide was added, a few mg at a time, and the specific gravity of the mixture was determined by dividing the mass of the mixture by its volume. Hence tungsten carbide was added until a specific gravity of 4.2 was achieved. The mixture could not have a greater specific gravity than

this because if more tungsten carbide were added, it started clumping up and settling out on the bottom of the container.

Since the colloidal mixture had a tendency to settle out fairly easily, the mixture was pipetted into 1.5 ml vials as soon as it was ready. It was relatively easy to shake the mixture back to its colloidal form if any settling took place.

Once the mixture had been prepared and pipetted out into 1.5 ml vials, the sample was poured into it. A vigorous shaking ensured the mixing of the sample and avoidance of any settling of the mixture. The separation was allowed to take place for fifteen minutes.

After the separation had taken place, the contents of the vials were frozen with liquid nitrogen. The "intermediates" (non-magnetic particles with specific gravity between 3.0 and 4.2) which froze at the top of the colloid were washed off in a sieve of mesh size 10 microns. Tungsten carbide is a very fine grain powder which washed off with distilled water through the sieve. The sample grains were all larger than 10 microns in size, and there was no loss of sample through the sieve. The same procedure was adopted for the heavy non-magnetic fraction of the sample after it had thawed. In this step the tungsten carbide and sodium

polytungstate were thoroughly washed off with distilled water to reduce contamination in the sample. After washing, the samples were dried in an oven at 80 °C for twelve hours (or overnight).

The samples were weighed and the weights were recorded. It was endeavored to weigh the samples at every separation step, so that the zircon content can be determined as a fraction of the bulk sample. This would help in determining the economic value of zircon in the beach sands.

2.2.5 Terminology

Since the samples underwent several separation steps which need to be referenced later, different fractions of the samples were named for convenience. The "bulk sample" was the sand as collected from the beaches. The "lights" referred to the fraction which had a specific gravity of less than 3.0. The "heavy fraction" was that portion which had specific gravity greater than 3.0, but had magnetic as well as non-magnetic portions of the samples. The "intermediates" were the non-magnetic portion with specific gravity less than 4.2. The non-magnetic fraction of the bulk samples with specific gravity greater than 4.2 were designated the heavy non-magnetic (HNM) fraction. Henceforth this terminology is adopted throughout this

report.

2.3 SAMPLE MASSES

The samples, as they progressed through the sample preparation techniques, were weighed at every step. This was required to calculate the fraction of each element present in the bulk samples. The following samples were weighed at all the separation steps: Moonstone, Nesika, Manzanita, Roads End, Crescent City, North Fern Canyon and Beach #3. Table 2 gives the masses of the samples at various stages of separation.

The following samples were obtained from the College of Oceanography after the 3.0 specific gravity separation had taken place: Cape Blanco, Sacci, Heceta, Agate, Ocean Beach, Meriweather, Hunters Cove and Port Orford. Bulk mass data were not available for these samples.

After the separation at a specific gravity of 3.0 was completed, the data from all the samples were combined. Tables 3 and 4 give the masses of all the samples at the magnetic separation and 4.2 specific gravity separation stages.

After the separation was completed, the intermediate and heavy non-magnetic fractions of the samples were examined under a microscope. The HNM

TABLE 2

Masses (g) of selected samples at various stages of separation.

SIEVING

Sample	Bulk	Coarse fraction	Fine fraction
Moonstone	42.52	8.25	33.55
N. Fern Canyon	58.60	9.22	49.14
Crescent City	83.23	3.60	79.40
Nesika	61.20	38.35	22.55
Roads End	66.60	50.00	16.50
Manzanita	162.05	136.90	25.10
Beach #3	92.55	0.00	92.51

SEPARATION OF FINE FRACTION AT SPECIFIC GRAVITY = 3.0

Sample	Light (< 3.0) fraction	Heavy (>3.0) fraction
Moonstone	31.8238	2.1045
N. Fern Canyon	0.4534	48.6634

Crescent City	21.3009	57.5684

TABLE 2 (continued)

Nesika	7.6102	14.5388
Roads End	8.0933	8.2673
Manzanita	17.9414	7.1660
Beach #3	38.7100	53.1000

MAGNETIC SEPARATION OF HEAVY FRACTION

Sample	Magnetic	Non-magnetic
Moonstone	2.0599	0.0323
N. Fern Canyon	48.0802	0.4039
Crescent City	56.8751	0.3583
Nesika	14.4192	0.0947
Roads End	8.2132	0.0576
Manzanita	7.0991	0.0560
Beach #3	43.7475	9.3030

TABLE 3

Masses of the samples after magnetic separation of the fine fraction of the bulk sample

Sample	Masses (g)	
	Before	After (non-magnetic)
Moonstone	32.6566	0.0429
N. Fern Canyon	49.4962	0.4594
Crescent City	62.1726	0.4499
Hunters Cove	7.5696	0.1176
Nesika	18.1666	0.1141
Port Orford	5.1529	0.4248
Cape Blanco	3.0376	0.1077
Sacci	9.3492	0.9862
Heceta	6.6954	0.1197
Agate	8.3312	0.8850
Roads End	13.7319	0.0992
Meriweather	6.5003	0.4526
Manzanita	8.9282	0.0738
Ocean Beach	5.6693	0.1121
Beach #3	51.1000	9.3030

TABLE 4

Masses of the intermediate and HNM fractions of the non-magnetic samples after separation at specific gravity = 4.2

Sample	Intermediate (g)	HNM (g)
Moonstone	0.0297	0.0082
N. Fern Canyon	0.0719	0.3765
Crescent City	0.2167	0.1626
Hunters Cove	0.0686	0.0520
Nesika	0.0725	0.0279
Port Orford	0.0398	0.3751
Cape Blanco	0.0195	0.0825
Sacci	0.0408	0.4867
Heceta	0.0392	0.0677
Agate	0.1832	0.6664
Roads End	0.0326	0.0515
Meriweather	0.1008	0.3403
Manzanita	0.0200	0.0432
Ocean Beach	0.0651	0.0270
Beach #3	0.2343	0.4471

fraction of the samples was counted for zircon using the standard petrographic analysis method [12], and was found to consist mainly of zircon. The intermediates were examined for their general composition. Tables 5 and 6 show the results of the microscopic examination of the intermediate and heavy part of the samples.

2.4 SAMPLE ENCAPSULATION

2.4.1 Polyvial sizes.

Encapsulation for irradiation was the final step in sample preparation. After the zircon samples had been separated, they were triply encapsulated in polyethylene polyvials for the purpose of irradiation and to safeguard the sample from spilling if any of the heat seals on the polyvials broke. For this objective polyvials of sizes 2 drams, 2/5 dram and 2/27 dram were chosen. Since the mass of the sample was not to exceed 160 mg (this upper limit for mass is determined on the basis of activity produced in the sample), 2/27 dram polyvials were appropriate for the inner sample encapsulation.

2.4.2 Decontamination procedure for polyvials.

The vials were decontaminated before the samples were placed in them. This was achieved by putting the

TABLE 5

The composition of the samples retained as the intermediate part

Sample	Description
Moonstone	Not examined
N. Fern Canyon	Mostly garnet
Crescent City	A few percent zircon
Hunters Cove	Opaques and rock fragments
Nesika	Pyroxine, rock fragment
Port Orford	Over 50% zircon
Cape Blanco	< 5% zircon, rock fragments
Sacci	10 - 15% zircon, garnet and rock fragments
Heceta	20% zircon
Agate	Clear garnet, 20% zircon
Roads End	Mostly clear pyroxine
Meriweather	20 - 30% zircon, garnet and pyroxine in equal parts
Manzanita	Mostly pyroxine and rock fragment
Ocean Beach	90% clear pyroxine
Beach # 3	40% zircon, 60% garnet

TABLE 6

Petrographic analysis (percent composition) of the HNM samples.

Sample	Zircon	Garnet	Opaques	Rutile	OH
Moonstone	89	1	6	4	0
N. Fern Canyon	90	0	6	4	0
Crescent City	96	0	3	1	0
Hunters Cove	99	0	1	0	0
Nesika	94	0	3	3	0
Port Orford	96	0	1	3	0
Cape Blanco	93	2	4	1	0
Sacci	97	0	3	0	0
Heceta	98	0	1	1	0
Agate	100	0	0	0	0
Roads End	90	0	3	7	0
Meriweather	99	0	0	1	0
Manzanita	21	0	2	0	77
Ocean Beach	94	0	2	4	0
Beach # 3	99	0	1	0	0

Note: OH = Other heavies

vials in a large beaker filled with ethyl alcohol. The beaker was then placed in an ultrasound bath for fifteen minutes. After washing with alcohol, the vials were rinsed with distilled water and then washed with 15% nitric acid in the ultrasound. This procedure eliminated any organic and inorganic impurities clinging to the polyvials. To avoid further contamination afterwards, the polyvials were handled with gloves and always placed on clean surfaces.

2.4.3 Polyvials sealing and spacers.

The samples were weighed and sealed into 2/27 dram polyvials. A quartz rod was used for heat sealing the small vials. These vials were placed in 2/5 dram polyvials which were then placed in 2 dram polyvials. To secure the vials, empty polyvials or spacers were placed in the 2 dram and 2/5 dram polyvials. The spacers would also hold secure the lid of the polyvials containing the sample inside it, in case the heat seal broke during irradiation of the sample.

The samples were then ready for irradiation.

3. METHOD OF ANALYSIS

3.1 PRINCIPLES OF INSTRUMENTAL NEUTRON ACTIVATION ANALYSIS

The basic principle involved in neutron activation analysis (NAA) starts with the fact that, when the atoms of a particular element are bombarded with neutrons, there is a definite probability associated with the nucleus of the atom that the neutron would be absorbed. The nucleus becomes radioactive by the absorption of the neutron and can have several different modes of decay. When the decay of the nucleus takes place by the emission of a γ-ray, then the absorption of the neutron is known as radiative capture. The γ-ray emitted by the nucleus has a unique energy and can be considered as the signature of that particular atom.

Neutron activation analysis is based on the identification of elements present in a sample after it has been irradiated by a neutron source, such as a nuclear reactor. The energy of the γ-ray and the area of the associated photopeak are used to determine the amount of that element in the sample [17]. The potential use of neutrons to analyze unknown samples was realized as early as 1936 [18].

The method of instrumental neutron activation analysis (INAA) was used in this project to analyze the zircon samples. INAA has been developed over the years as a major tool in sample analysis. INAA has been successfully used for the analysis of a wide variety of samples, such as geological, lunar, chemical and industrial samples. With the advances in technology which have produced better electronic instruments as well as more efficient detectors which work in conjunction with readily available personal computers and versatile software, INAA has become a powerful method for sample analysis which is used all over the world.

3.2 INAA PARAMETERS

3.2.1 Standards.

In this project the comparative method for sequential neutron activation analysis was used to determine the elemental concentrations in a sample. For this method standards are required. Five standards were used for this purpose. These were the fly-ash (NBS 1633a), CRB (Columbia River Basalt), a U standard, a Zr standard, and a Mg standard. The first two of the standards are certified by the National Bureau of Standards (NBS) and the elemental concentrations are

available in several literature sources as well from NBS [19, 20]. Fly-ash and CRB were used in the form of a fine powder. The U and Zr standards were prepared in liquid form. The uranium standard contained a U concentration of 203 μg/ml and the zirconium standard had a Zr concentration of 9.95 mg/ml. The Zr standard also had Hf present in a concentration of 1.13 μg/ml. The Mg standard was also in liquid form and had a concentration of 2.3 mg/ml. These five standards were chosen on the basis of containing a wide variety of elements whose concentrations were verified several times over and were appropriate as standards for the expected elemental concentration levels in the zircon samples. Table 7 gives the elemental concentrations of the NBS1633 and CRB standards, and the Zr, U, and Mg standards.

3.2.2 Mass.

The quantity of a sample which is determined to be suitable for irradiation depends mostly on the elemental composition of the sample. If an approximate composition of the sample is known, and the sample consists mainly of elements which have a very high absorption cross section for neutrons, the activity induced in the sample would be high and it would require a longer decay period. For sequential neutron

TABLE 7

Elemental concentration of the INAA standards

Element	SRM 1633a	CRB	Zr	U
Ti (%)	0.79	1.32		
Al (%)	14.3	7.2		
Fe (%)	9.41	9.72		
Mn (%)	0.0179	0.141		
Mg (%)	0.452	2.08		
Ca (%)	1.107	5.00		
Na (%)	0.171	2.44		
K (%)	1.875	1.41		
Sc (ppm)	39.9	32.8		
V (ppm)	297	404		
Cr (ppm)	193	13.6		
Co (ppm)	43.1	36.3		
Zn (ppm)	220	107		
Se (ppm)	10.3	0.086		
Rb (ppm)	134	58		
Sr (ppm)	835	330		
Sb (ppm)	6.8	0.13		
Cs (ppm)	10.42	1.3		
Ba (ppm)	1340	680		

TABLE 7 (continued)

Element	SRM 1633a	CRB	Zr	U
La (ppm)	79.1	25		
Ce (ppm)	168.3	54		
Nd (ppm)	75.7	29		
Sm (ppm)	16.83	6.58		
Eu (ppm)	4	1.96		
Tb (ppm)	2.38	1.05		
Dy (ppm)		6.4		
Yb (ppm)	7.5	3.4		
Lu (ppm)	1.075	0.51		
Zr (ppm)	240	191	9920	
Hf (ppm)	6.9	4.6	1.13	
Th (ppm)	24	6		
U (ppm)	10.3	1.7		203

activation analysis this would not be advantageous as the short-lived nuclei would decay by the time the sample was safe enough to be handled. On the other hand, the sample should not be so small in mass that the activity induced in the sample would give so few counts in the photopeak that it would lead to poor counting statistics and results.

In this project the samples had masses in the range of 20 - 160 mg, although there was one sample with a mass of less than 10 mg since that was all of the material available. A preliminary calculation was carried out for all samples to calculate the induced activity due to expected major nuclides. Table 8 gives the final masses of the samples which were irradiated.

3.2.3 Neutron Flux.

The samples and the standards are often irradiated under identical neutron flux conditions for INAA. In this project the Oregon State University (OSU) TRIGA Reactor (OSTR) at the OSU Radiation Center was used for irradiating the samples. For both long and short irradiations the reactor was operated at a power level of 1 MW, which gave a flux of 9×10^{12} n/cm^2-s in the pneumatic transfer system, and a flux level of 3×10^{12} n/cm^2-s at the rotating rack. The mass of the samples combined with this flux level gave a count rate which

TABLE 8

Final masses of the irradiated samples

Sample	Mass (g)
Moonstone	0.0073
N. Fern Canyon	0.1398
Crescent City	0.1559
Hunters Cove	0.0451
Nesika	0.0247
Port Orford	0.1532
Cape Blanco	0.0808
Sacci	0.1301
Heceta	0.0649
Agate	0.1503
Roads End	0.0507
Meriweather	0.1487
Manzanita	0.0430
Ocean Beach	0.0203
Beach # 3	0.1491

produced satisfactory statistics for most of the nuclides of interest.

3.2.4 Irradiation, decay and counting times.

Irradiation, decay and counting times are very important factors in sequential NAA [21]. Sequential neutron activation analysis follows the procedure of counting the short-lived radionuclides first, followed by a decay period and subsequent counting of the longer-lived radionuclides.

For short irradiations the samples were irradiated in the pneumatic transfer facility of the OSTR for 2 minutes and then were allowed to decay for 10 minutes (an average time of 10 minutes was required to transfer the samples to clean polyvials and transport them to the counting room). The short-lived radionuclides (representative of the elements Ti, Al, V, Mg and Ca) which had a half life in the range of 2 - 10 minutes were counted first. The first counting time was of 5 minutes duration. The samples and the standards were then allowed to decay for 3 hours so that the activity level of the short-lived nuclides was negligible. The decay of these short-lived nuclides reduced the Compton continuum for the photopeaks of the longer-lived radionuclides. These samples were then counted for 10 minutes for the elements Dy, Na, K and Mn.

For the long irradiations, the samples and the standards were irradiated for 7 hours in the rotating rack (Lazy Susan) of the OSTR. The samples were allowed a decay period of 7 days which was sufficient for the short-lived radionuclides to decay completely away. The samples were then counted for 3 hours for the elements Fe, Co, As, Sb, Rb, Ba, La, Nd, Sm, Yb, Lu, W, and Np. The radionuclides associated with these elements were allowed to decay for 30 days and then the radionuclides associated with the elements Sc, Cr, Co, Zn, Se, Sr, Sb, Cs, Ce, Eu, Tb, Zr, Hf, Ta, and Pa were counted for 6 hours.

Table 9 gives properties of the radioisotopes to be measured along with some other parameters of this analysis [21]. These are the elements which are most likely to be found in a geological sample.

3.3 SAMPLE IRRADIATION AND HANDLING PROCEDURES

3.3.1 Pneumatic transfer facility.

For irradiation in the pneumatic transfer facility the reactor power level was 1 MW. The samples and the standards were placed one at a time in polyethylene "rabbit" polyvial, and irradiated for a period of 2 minutes. After irradiation, the sample was checked for exposure rate which should not be greater than 500

TABLE 9

Radionuclides and INAA parameters.

Isotope	Half life	γ-ray energy (keV)
	Group A	
^{51}Ti	5.79 min	320
^{27}Mg	9.46 min	1014
^{52}V	3.75 min	1434
^{28}Al	2.32 min	1779
^{49}Ca	8.80 min	3084
	Group B	
^{165}Dy	2.32 hr	95
^{56}Mn	2.58 hr	847, 1811
^{24}Na	15.0 hr	1369
^{42}K	12.4 hr	1524
	Group C	
^{59}Fe	44.5 day	1099, 1292
$^{58}Ni(^{58}Co)$	71.3 day	811
^{86}Rb	18.7 day	1077

TABLE 9 (continued)

Isotope	Half life	γ-ray energy (keV)
^{131}Ba	12.1 day	216, 496
^{140}La	40.2 hr	816, 1597
^{147}Nd	11.1 day	91, 531
^{153}Sm	46.8 hr	103
^{175}Yb	4.21 day	283, 396
^{177}Lu	6.74 day	208
^{238}U (^{239}Np)	2.36 day	106, 278
	Group D	
^{46}Sc	83.85 day	889, 112
^{51}Cr	27.8 day	320
^{65}Zn	243 day	1116
^{85}Sr	64 day	514
^{124}Sb	60.3 day	564, 1691
^{134}Cs	2.05 a	796
^{141}Ce	32.5 day	146
^{152}Eu	12.7 a	122, 1408
^{160}Tb	72.3 day	299, 879
^{95}Zr	64.02 day	756
^{181}Hf	42.5 day	482
$^{232}Th(^{233}Pa)$	27 day	300, 311

TABLE 9 (continued)

Group A & B

Facility: Pneumatic Transfer ("Rabbit")

Power level = 1 MW (ϕ = 9 x 10^{12} n/cm^2-s)

Irradiation time = 2 min

Decay time group A = 10-15 min

Counting Time = 5 minutes

Decay time group B = 2-5 hr

Counting Time = 10 minutes

Group C & D

Facility; Rotating Rack ("Lazy Susan")

Power Level = 1 MW (ϕ = 3.0 x 10^{12} n/cm^2-s)

Irradiation time = 7 hr

Decay time group C = 7 - 14 days

Counting Time = 3 hr

Decay time group D = 30 - 45 days

Counting Time = 6 hr

mR/hr. The sample was then transferred to a clean polyvial and taken to the counting laboratory. Transfer to a clean polyvial prevents spread of contamination.

3.3.2 Rotating rack.

The samples and the standards were placed in polyethylene "TRIGA" tubes in the rotating rack and irradiated for 7 hours at a steady power level of 1 MW. The rack rotates at the rate of 1 revolution/min to ensure an identical exposure for all the samples. After irradiation the samples were placed in a Pb-lined cave for a week to reduce the dose rate to a safe level. This also allowed the short-lived radionuclides to decay to negligible levels. The samples were then transferred to clean polyvials. When the samples were being transferred, care was taken that the clean polyvials did not get contaminated. The samples were then transferred to the counting laboratory.

3.4 COUNTING SYSTEM AND DATA ANALYSES

3.4.1 Detector and NIM electronics.

The data were collected using a PGT (Princeton Gamma Tech) Ge(Li) detector and its associated electronics (see Fig. 3). A multichannel analyzer (ORTEC 918A) with a buffer collected and stored all the

data for the samples.

The p-type Ge(Li) detector, with a 13% efficiency (relative to a 7.62 cm by 7.62 cm NaI(Tl) detector at 1332 keV), was employed to count the samples and the standards. The peak to Compton ratio of the detector was 47:1 at 1332 keV. A Ge(Li) detector has several advantages such as extremely good energy resolution and a linear energy response that is independent of the particle type. These advantages far outweigh the disadvantage of a somewhat lower detection efficiency when the purpose is the simultaneous detection of several elements in a sample [22].

In this counting system the Ge(Li) detector was accompanied by a high voltage power supply (ORTEC 459), a preamplifier (PGT RG-11), an amplifier (ORTEC 572), a counter/timer (Canberra 1776)and a multichannel analyzer (MCA). The MCA was used in conjunction with a Leading Edge Model D PC. The counting system configuration also is shown in Fig. 3.

3.4.2 Efficiency calibration.

The counting system must be calibrated for data reduction. A Eu-152 source was used to calibrate the system for data reduction of the short irradiation samples. For the long irradiation samples, the NBS fly-ash standard was used to calibrate the system. Fig. 4

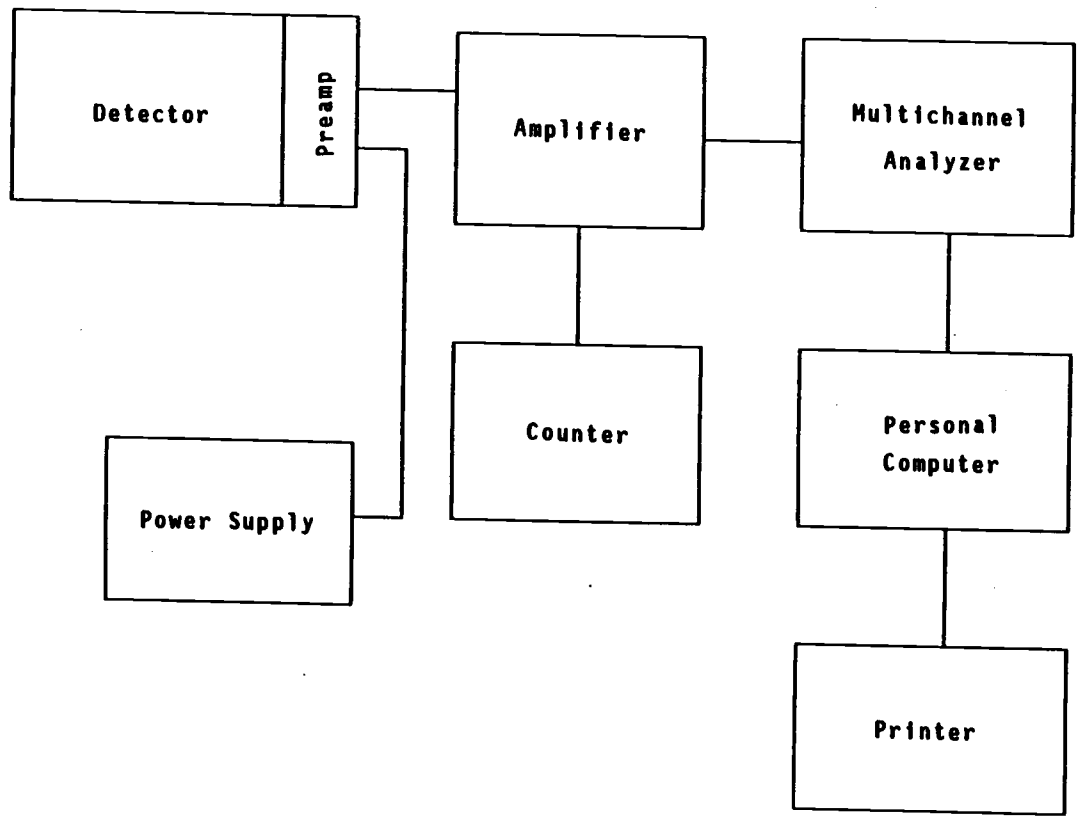

Fig. 3. Counting system configuration

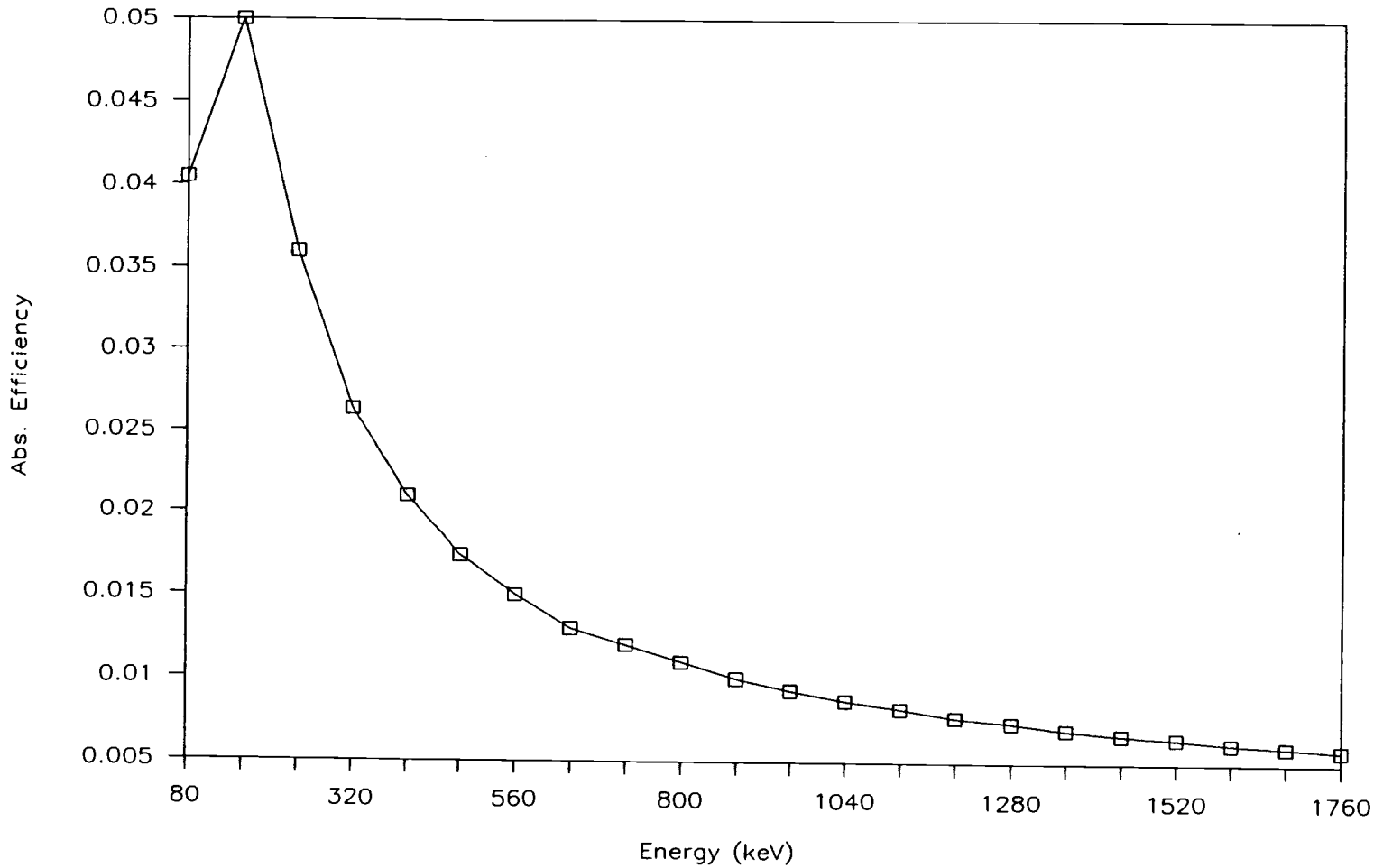

Fig. 4. Efficiency curve for Ge(Li) detector

shows the calibration curve obtained from the Eu-152 source, placed 7.5 cm away from the detector. The efficiency curve spans an energy range of 80 - 1760 keV, which covers most of radioisotopes measured.

3.4.3 Data reduction.

For the data obtained from the short irradiation counts of 5 minutes, a Lotus 1-2-3 program was used to calculate the percent composition for the major and minor elements and the ppm concentrations in the case of the trace elements. This program, developed at OSU, uses the equations shown in Appendix B.

The data obtained for the counting times of 10 minutes, 3 hours, and 6 hours were reduced with an EG&G ORTEC software program known as GELIGAM, version 2.05. The program also uses the equations given in Appendix B. The decay of the radionuclide during counting and the dead time of the detector were accounted for in the program.

The Lotus 1-2-3 program was used for the short counts of five minutes because GELIGAM does not handle radionuclides with <10 minutes half life.

4. RESULTS

The separation method worked fairly well in most of the samples, the zircon percentage being in the range of 70 - 95% by weight in the HNM fraction, as determined by INAA results. It must be mentioned here that the sample from Manzanita Beach consisted of mostly rock fragments and did not have the same general composition as the rest of the samples; therefore it is not included in any further discussion. The following results are based on actual sample masses of the heavy non-magnetic fractions of the bulk samples.

Table 10 shows the weight percent of the major and minor elements in the HNM samples. From the data collected, Zr was the major element with its abundance in the HNM samples being in the range of 16.55 - 47.22% by weight. The highest concentration of Zr (47.22%) occurred at Agate Beach (latitude = 44.67°). The maximum possible concentration of Zr in a pure zircon sample is 49.57%, the weight percentage of Zr in $ZrSiO_4$. The HNM fraction of Oregon beach samples were generally high in zircon content. Beach #3, which is in Washington, also had a high abundance of zircon (92.97%). Figure 5 shows the variation of zirconium as a function of latitude.

TABLE 10

Major and minor elements in the zircon samples (Percentages are by weight of zircon sample).

Sample	Ti (%)	Al (%)	Ca (%)	Zr (%)	Hf (%)	Ba (%)
Moonstone	28.24	0.88	1.99	16.55	0.37	2.10
N. Fern Canyon	28.75	0.20	0.48	21.07	0.47	0.19
Crescent City	12.89	0.72	0.78	35.94	0.74	*
Hunters Cove	15.55	0.56	0.68	38.03	0.84	1.67
Nesika	6.38	0.48	0.79	41.11	0.89	0.05
Port Orford	3.03	0.29	0.24	44.53	0.93	0.56
Cape Blanco	6.25	0.97	0.81	41.94	0.96	0.85
Sacci	2.56	0.29	0.09	43.60	0.92	*
Heceta	5.16	0.58	*	45.71	1.04	*
Agate	1.56	0.94	*	47.22	0.98	*
Roads End	2.96	6.50	0.88	39.03	0.89	0.28
Meriweather	2.46	0.53	0.20	44.24	0.92	*
Ocean Beach	8.13	5.64	2.48	28.98	0.67	*
Beach #3	2.18	0.20	0.37	46.28	1.00	0.15

Note: * concentration < 500 ppm

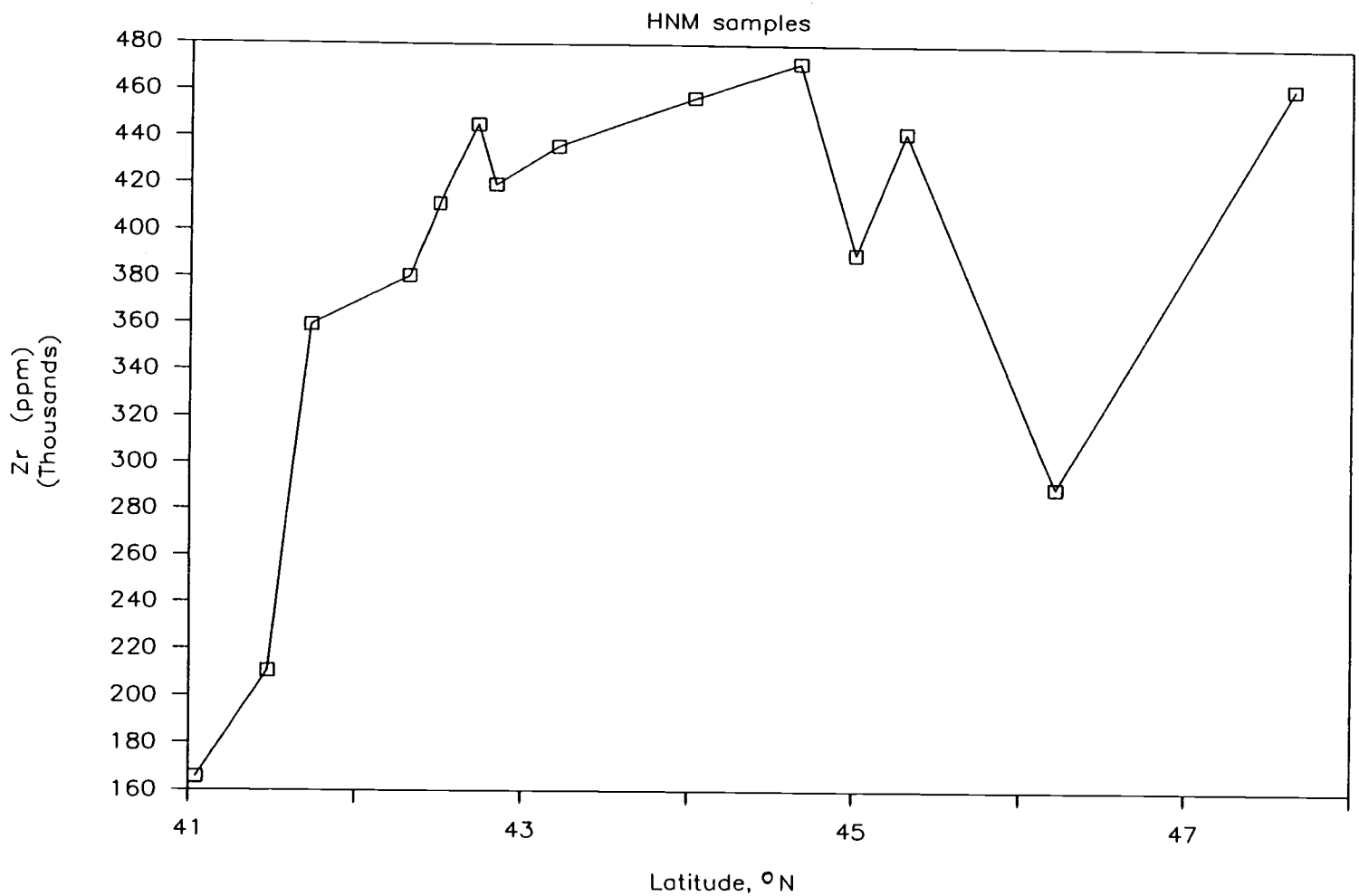

Fig. 5. Zirconium abundance versus latitude

Hafnium, which is always present with Zr in nature, generally followed the abundance trend of Zr in the samples, with its concentration increasing or decreasing with Zr. The abundance range of Hf was 3659 ppm to 10410 ppm. The percentage of Hf abundance to (Zr + Hf) abundance was calculated and the values fall in the range of 2.02 - 2.24 as shown in Table 11, with a mean and a standard deviation of 2.13 and 0.08, respectively. Figure 6 shows the variation of the Hf concentration with latitude, and Figure 7 shows the Hf abundance plotted as a function of Zr abundance. The linear relationship of the two elements can easily be inferred from Figure 7.

Titanium was the other principal element which showed up as a major element in the samples. The abundance of Ti in the samples ranged from 1.56 to 28.8%, the highest concentration of Ti occurring at the two southernmost beaches, Moonstone and N. Fern Canyon, where it was 28.2% and 28.8%, respectively. The next two beaches to the north, Crescent City and Hunters Cove, had an abundance of 12.9% and 15.6%, respectively. For rest of the samples the abundance of Ti was less than 10%. Figure 8 shows the variation of Ti as a function of latitude and Figure 9 shows the variation of Ti as a function of Zr concentration. From Figure 9 it appears there is an inverse linear

TABLE 11

Hafnium content of the HNM samples

Sample	Zr (ppm)	Hf (ppm)	$\frac{Zr}{Hf}$	$\frac{Hf}{(Hf+Zr)}$ (%)
Moonstone	165500	3659	45.23	2.16
N. Fern Canyon	210700	4673	45.09	2.17
Crescent City	359400	7409	48.51	2.02
Hunters Cove	380300	8385	45.35	2.16
Nesika	411100	8932	46.03	2.13
Port Orford	445300	9307	47.85	2.05
Cape Blanco	419400	9606	43.66	2.24
Sacci	436000	9191	47.44	2.06
Heceta	457100	10410	43.91	2.23
Agate	472200	9805	48.16	2.03
Roads End	390300	8891	43.90	2.23
Meriweather	442400	9199	48.09	2.04
Ocean Beach	289800	6652	43.57	2.24
Beach #3	462800	9978	46.38	2.11

TABLE 11 (continued)

Zr/Hf Ratio:

1st eight samples:	Mean =	46.15
	σ =	1.54
Last six samples:	Mean =	45.67
	σ =	1.97

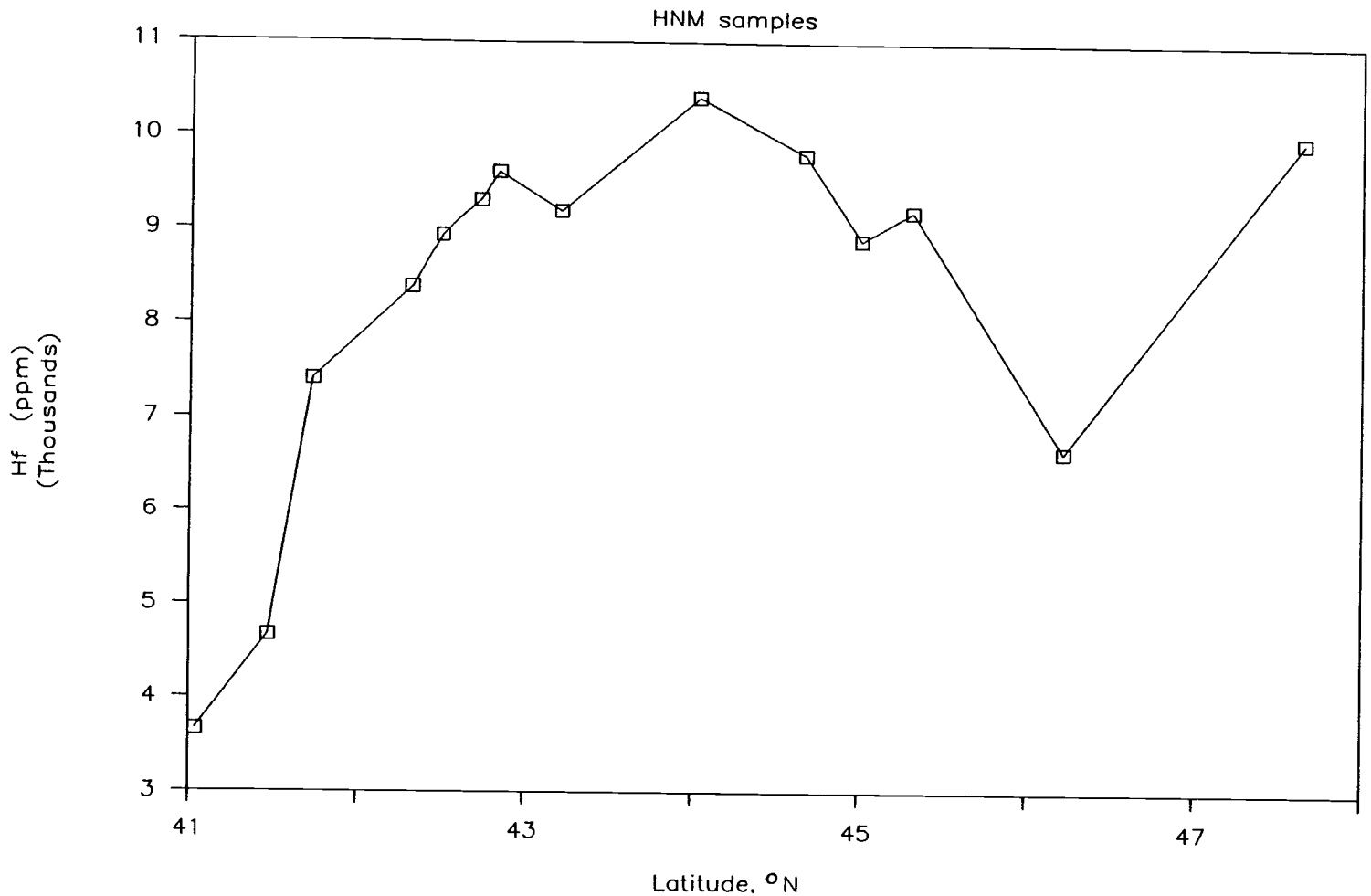

Fig. 6. Hafnium abundance versus latitude

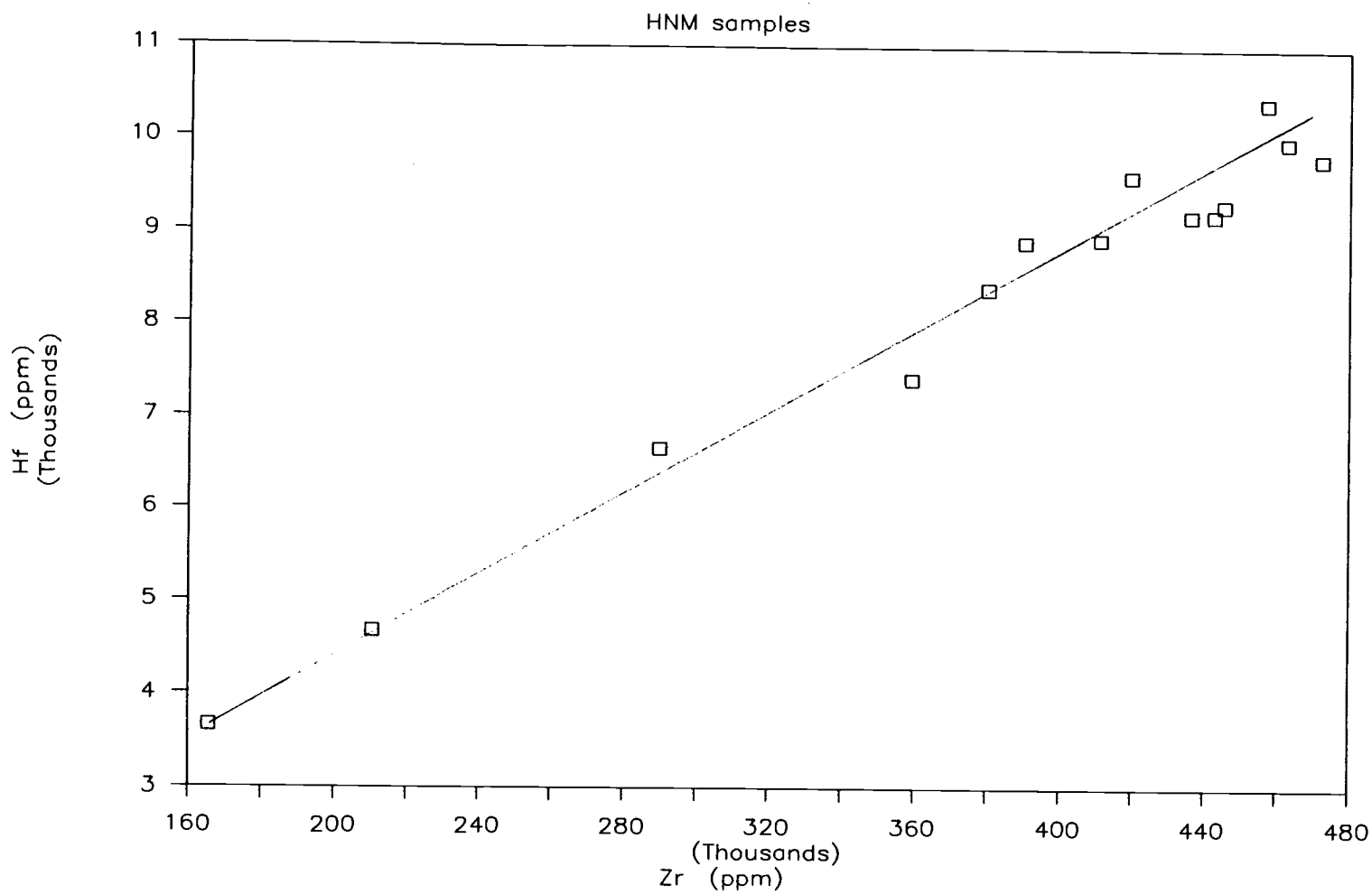

Fig. 7. Correlation between hafnium and zirconium abundances

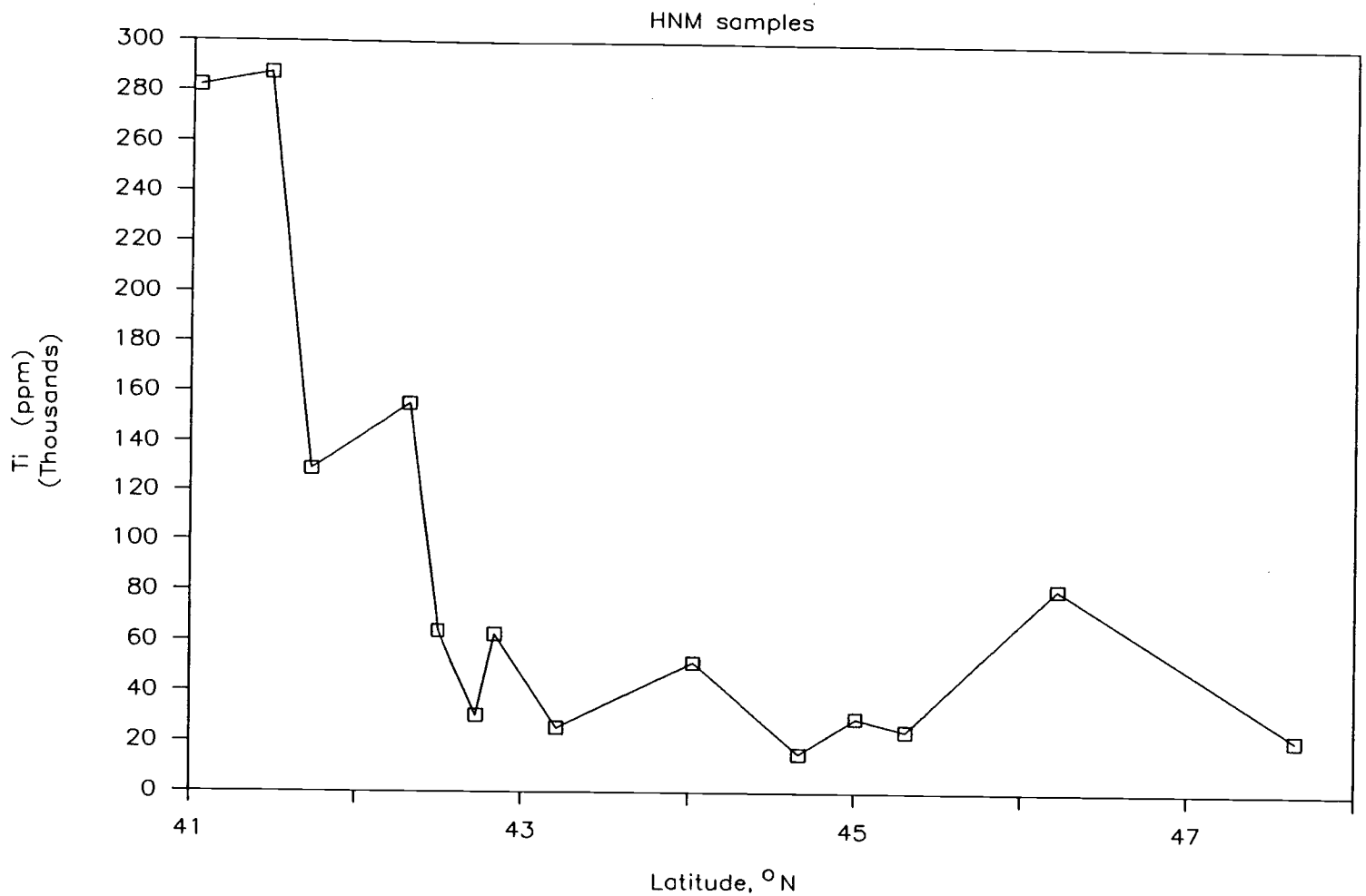

Fig. 8. Titanium concentration versus latitude

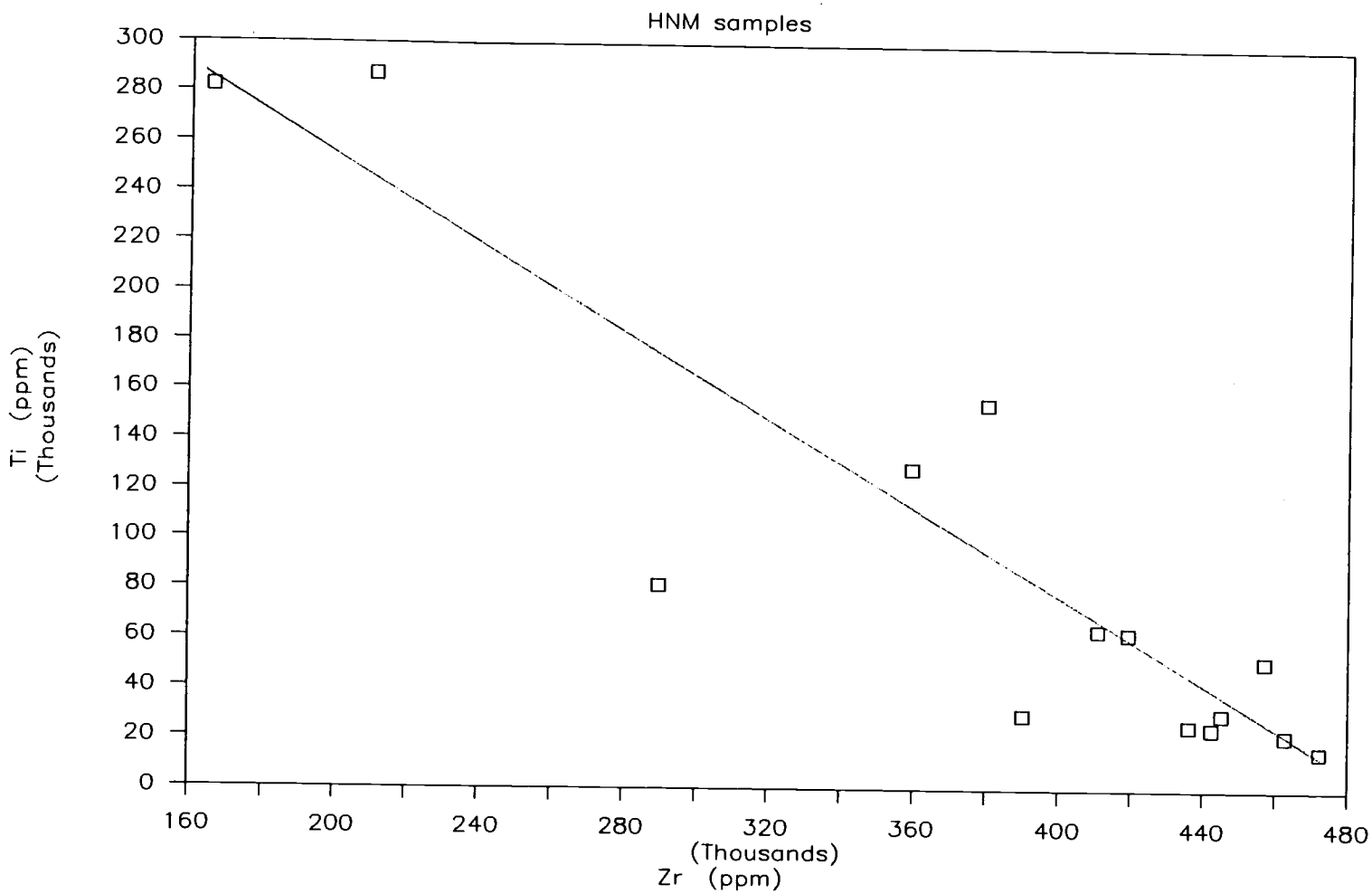

Fig. 9. Correlation between titanium and zirconium abundances

correlation between the abundances of these two elements, since as the amount of Ti in a sample decreases there is generally a corresponding increase in zirconium abundance. This trend can also be inferred from Figure 10, which shows the variation of Ti and Zr as a function of latitude. In the north, Ocean Beach has a relatively higher concentration (8.13%) of Ti, and correspondingly there is decrease in the Zr abundance in the sample. Figure 10 also shows the plot of Ti+Zr as a function of latitude, and it can be seen that the sum of the concentration of the two elements is fairly constant, spanning the Pacific coastline from Moonstone beach in northern California to Beach #3 in Washington.

The other elements which occurred as major elements in the zircon samples were Al, Mg and Ca. Aluminum occurred in the range of 0.20 - 6.5%. Calcium had an abundance range of 0.2 - 2.5% in 11 of the 14 samples. At Sacci Beach it was present only as a trace element with an abundance of 925 ppm. Heceta and Agate Beaches did not indicate any calcium above the upper concentration limit. Figures 11 and 12 show the variation of Al and Ca, respectively, as a function of latitude. Accurate amounts of Mg could not be determined in the samples.

Barium was one element which showed a highly varied range of occurrence, appearing as a major, minor or

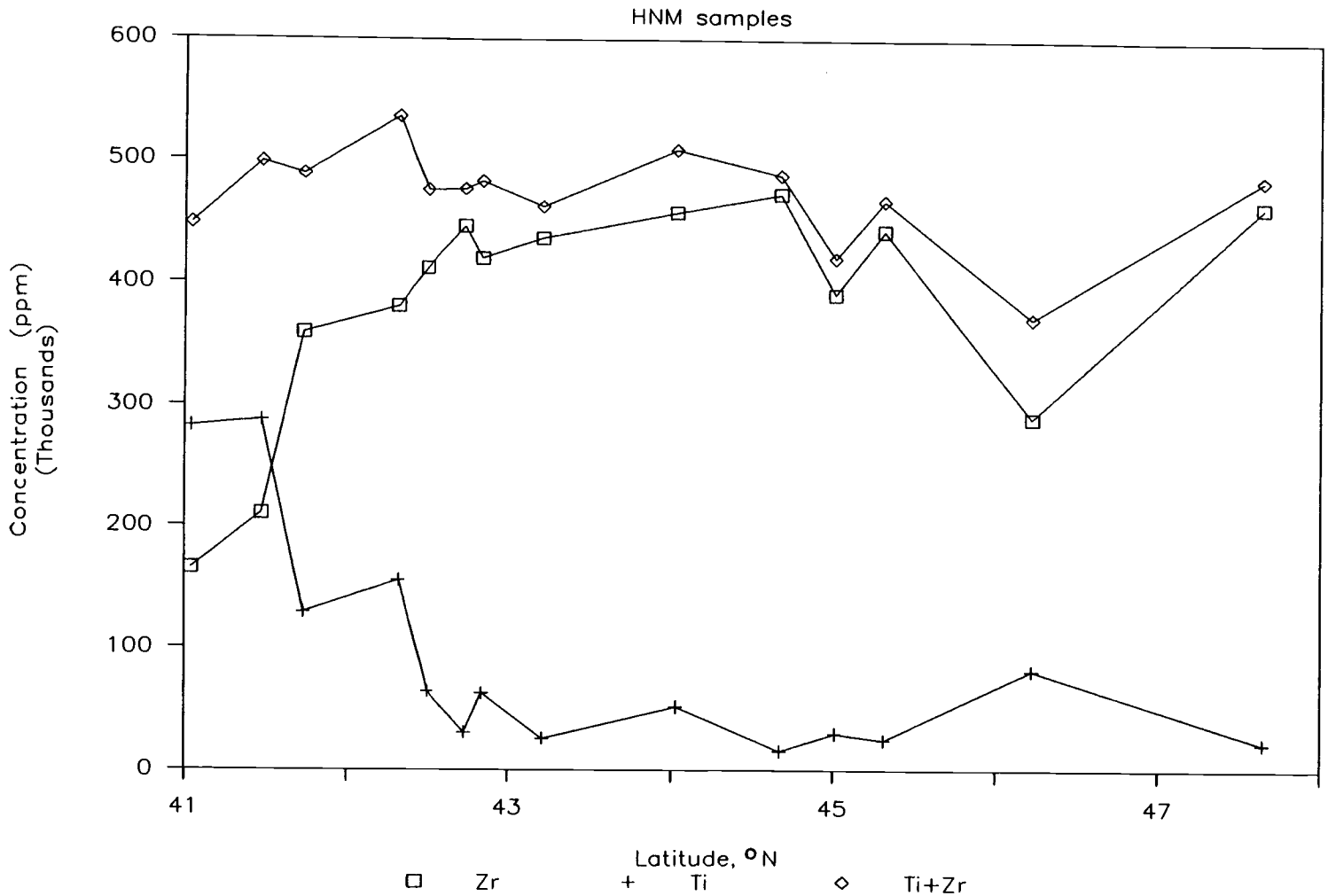

Fig. 10. Titanium, zirconium and Ti+Zr versus latitude

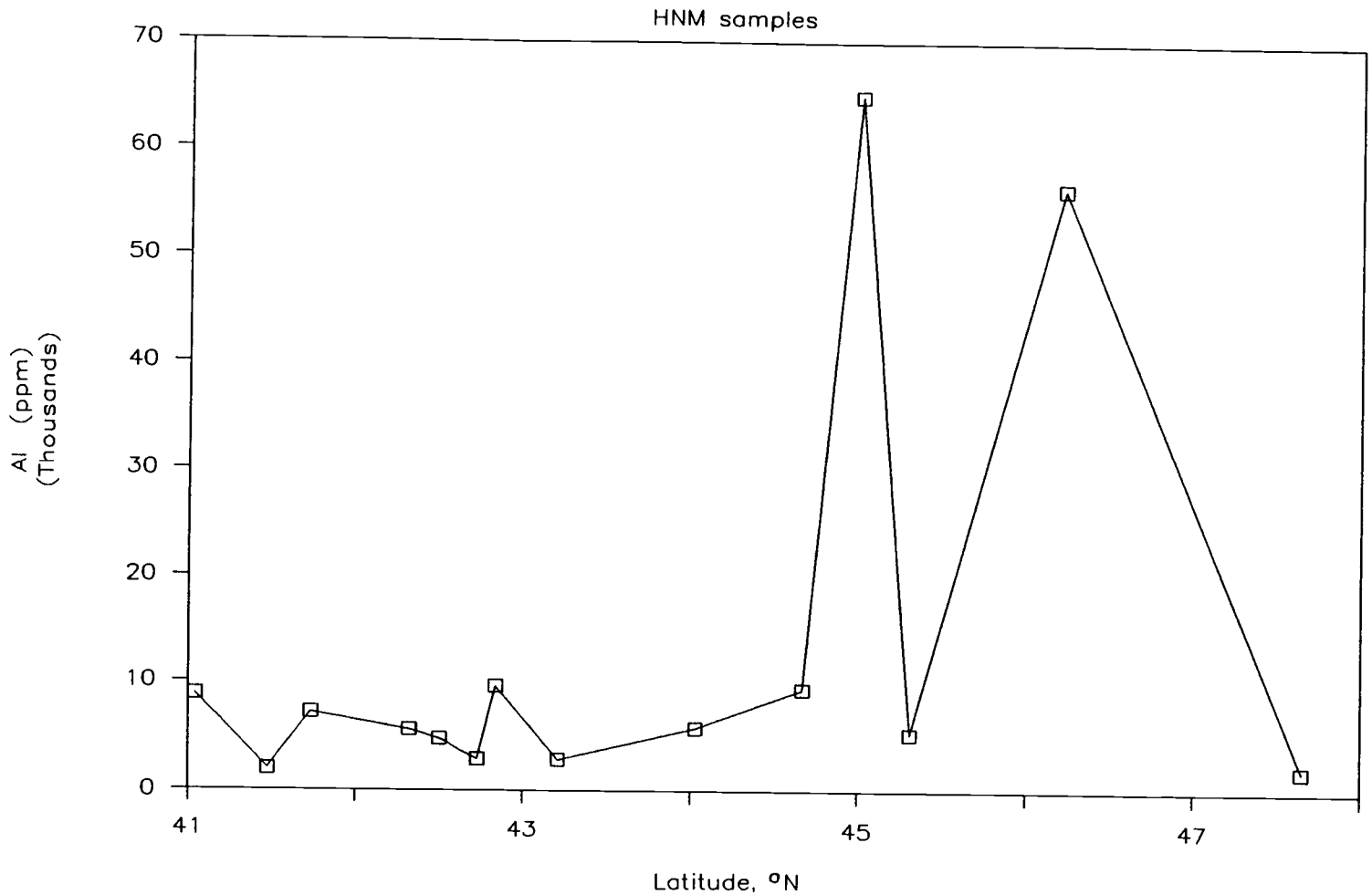

Fig. 11. Aluminum concentration versus latitude

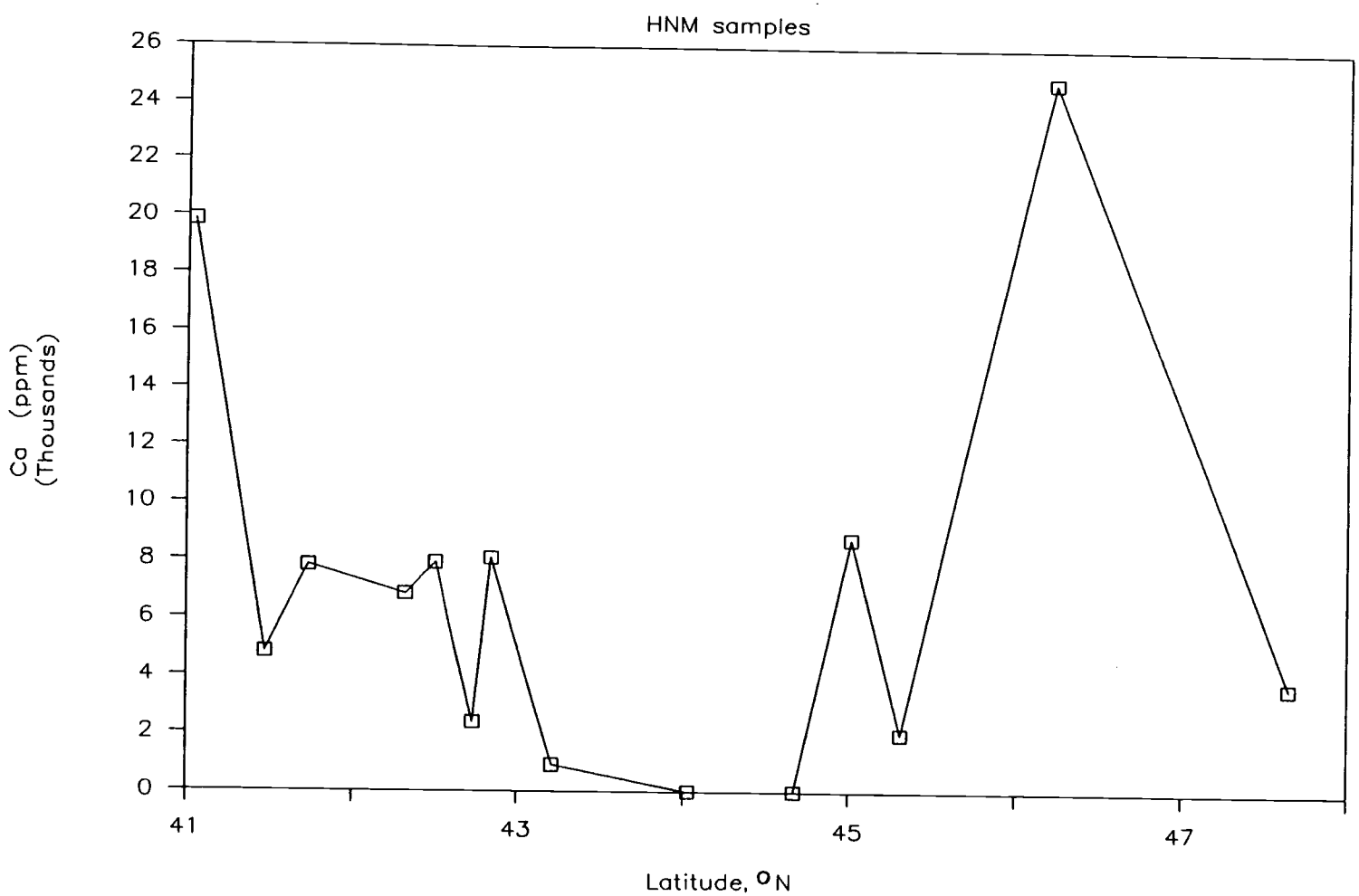

Fig. 12. Calcium abundance versus latitude

trace element in various samples. The abundance range of Ba was < 350 ppm (upper concentration limit) to 2.1% at Moonstone Beach. Figure 13 shows the Ba concentration versus latitude.

Table 12 shows the concentrations of the non-rare earth elements in the zircon samples. Vanadium occurs as a trace element in the samples, with a range of 50 - 655 ppm. Although V appears as a trace element, it follows a similar trend of occurrence as the major element Ti. The highest abundance of Ti was in the two beaches in the south, Moonstone and North Fern Canyon. The abundance of V in these two beaches was in excess of 650 ppm, while in all the other samples the V abundance was in the range of 50 - 320 ppm. Figure 14 shows the variation of V with latitude. Figure 15 shows the variation of V versus Ti concentration; the two elements seem to have a linear correlation.

Scandium and chromium occurred as trace elements in the HNM fraction. Scandium was present in the range of 39 to 79 ppm while Cr had range of occurrence between < 64 ppm and 343 ppm. Figures 16 and 17 shows the trend of abundances of Cr and Sc, respectively, as a function of latitude. The other non-rare earth elements present were: Zn (<1 - 302 ppm), Sb (<1 to 4 ppm), Cs (upper concentration limit in the range of 1 - 5 ppm), and Se (<1 - 55 ppm).

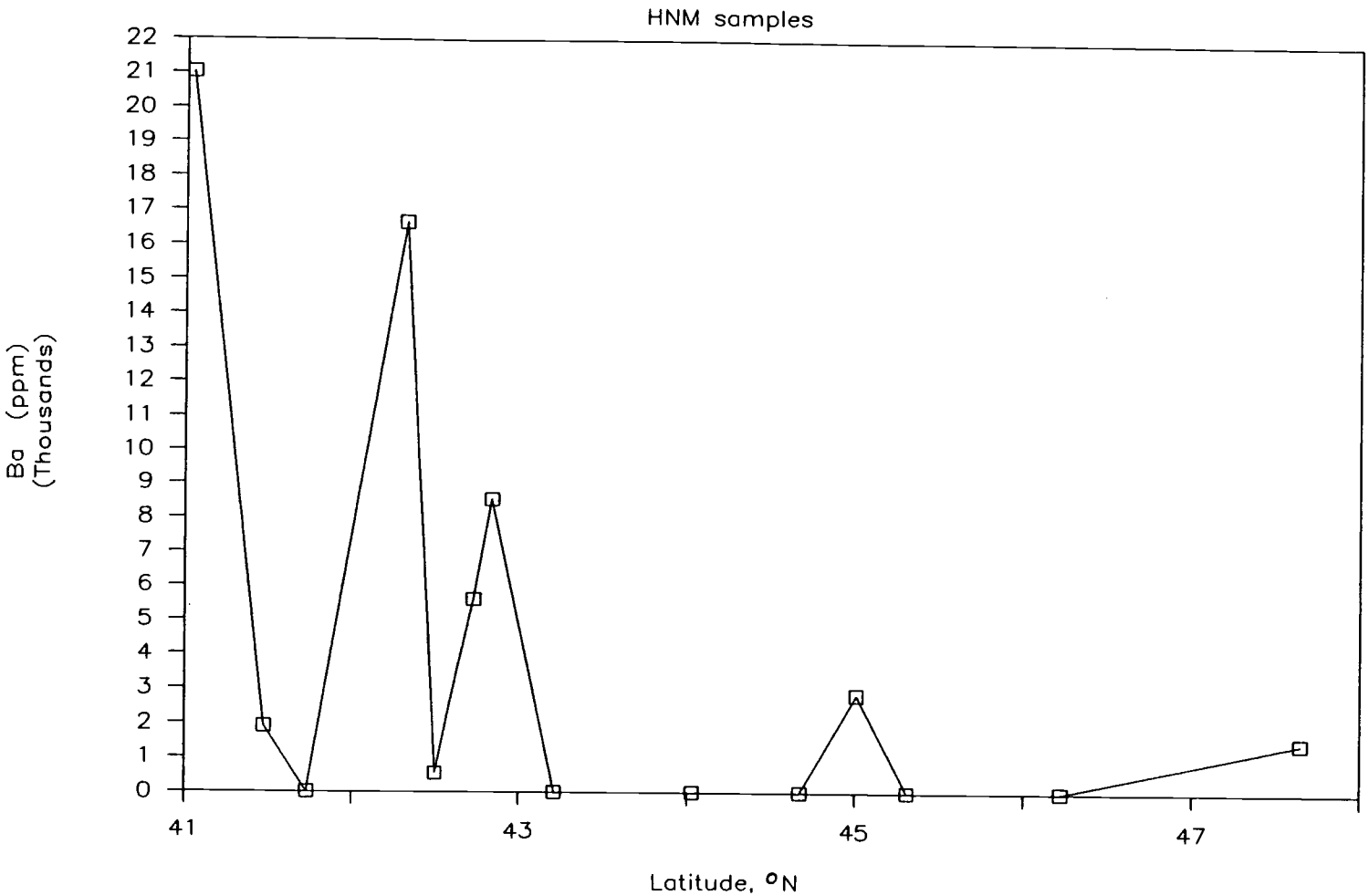

Fig. 13. Barium abundance versus latitude

TABLE 12

Selected trace element concentrations (ppm) in HNM samples

Sample	V	Sc	Cr	Zn	Sb	Cs	Se
Moonstone	664	75	172	<67	<4	<5	<37
N. Fern Canyon	661	39	343	<13	1	<1	55
Crescent City	175	77	153	*	1	<1	*
Hunters Cove	309	73	320	263	3	<2	28
Nesika	112	71	77	<3	<1	<2	<3
Port Orford	66	71	<64	*	1	<1	*
Cape Blanco	138	67	88	302	2	<1	43
Sacci	65	64	<74	*	1	<1	*
Heceta	130	68	93	244	2	2	43
Agate	52	68	<65	*	<1	<1	*
Roads End	120	57	73	192	2	<1	<2
Meriweather	79	64	167	*	1	<1	*
Ocean Beach	277	49	121	<41	4	<2	<29
Beach #3	56	79	<67	*	<1	<1	*

Note: * concentration could not be determined

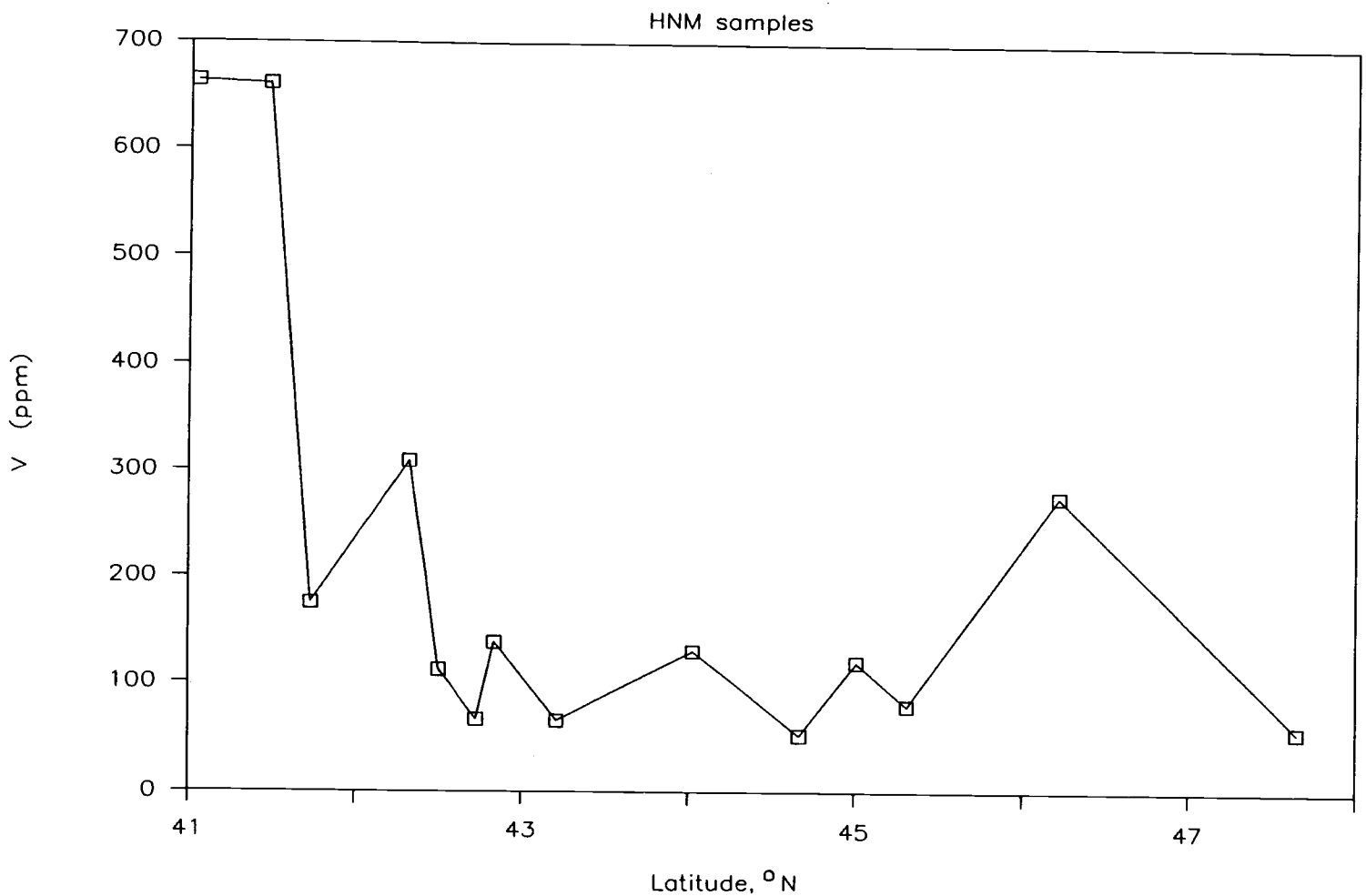

Fig. 14. Vanadium concentration versus latitude

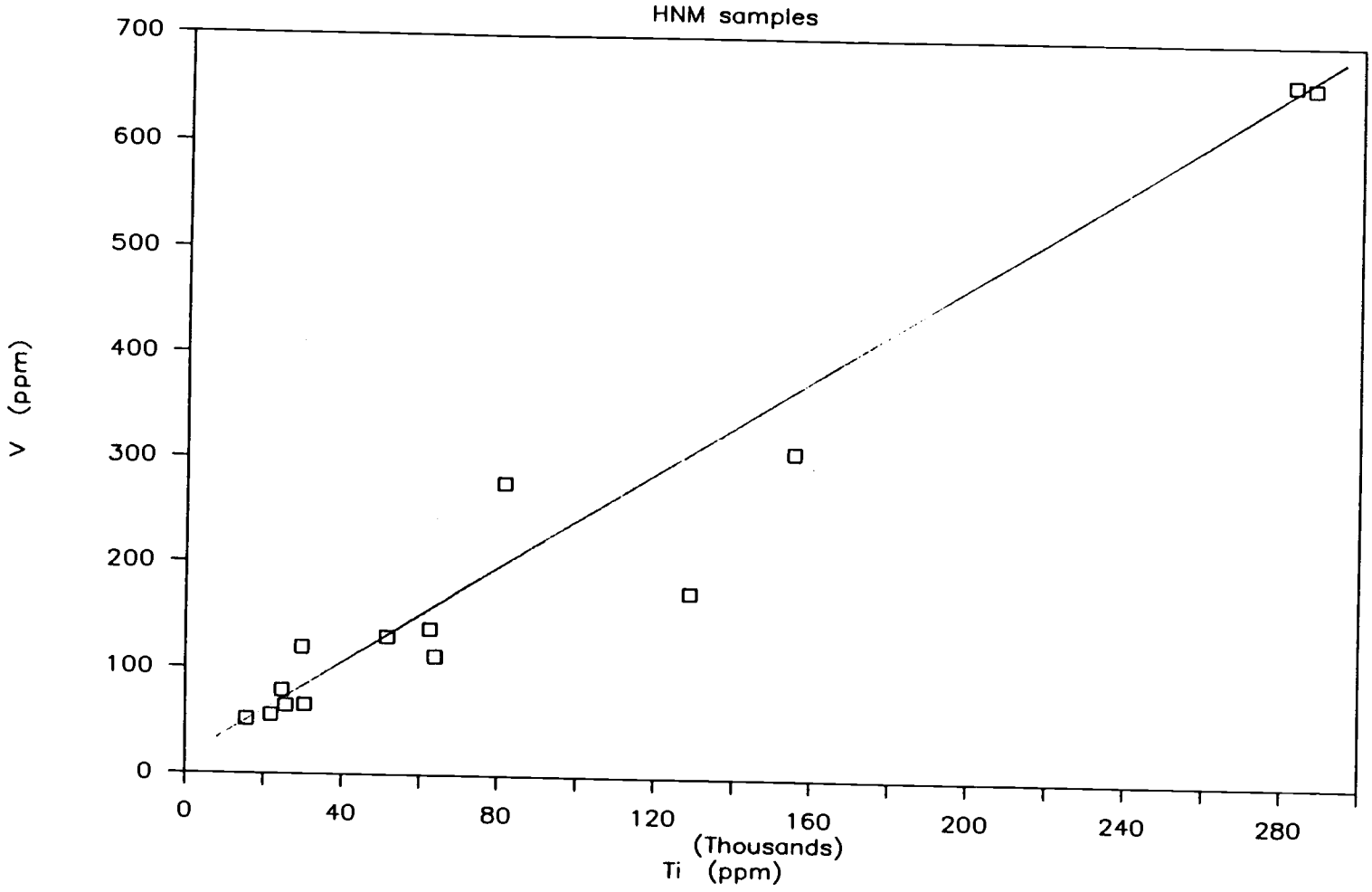

Fig. 15. Correlation between vanadium and titanium abundances

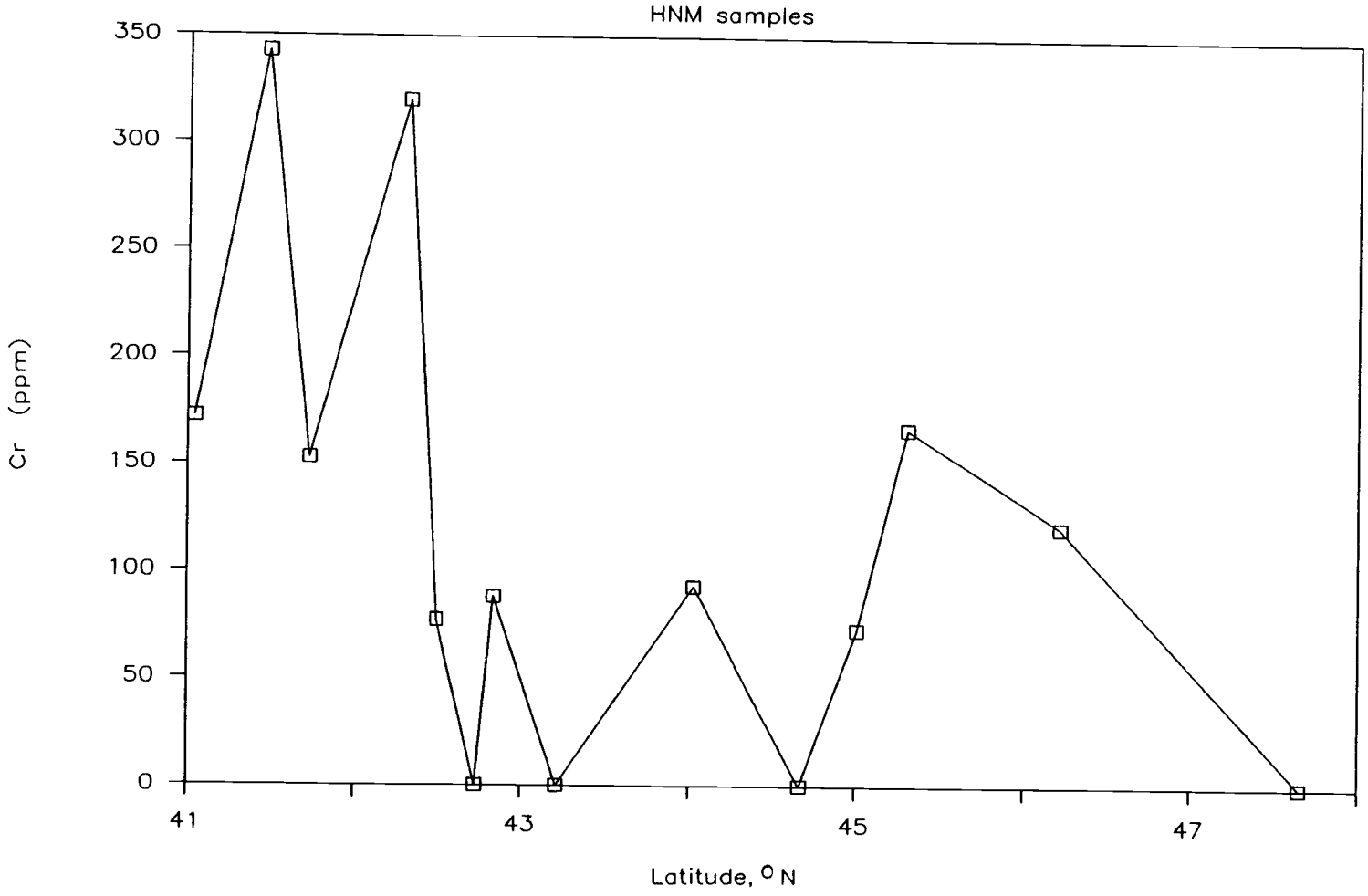

Fig. 16. Chromium concentration versus latitude

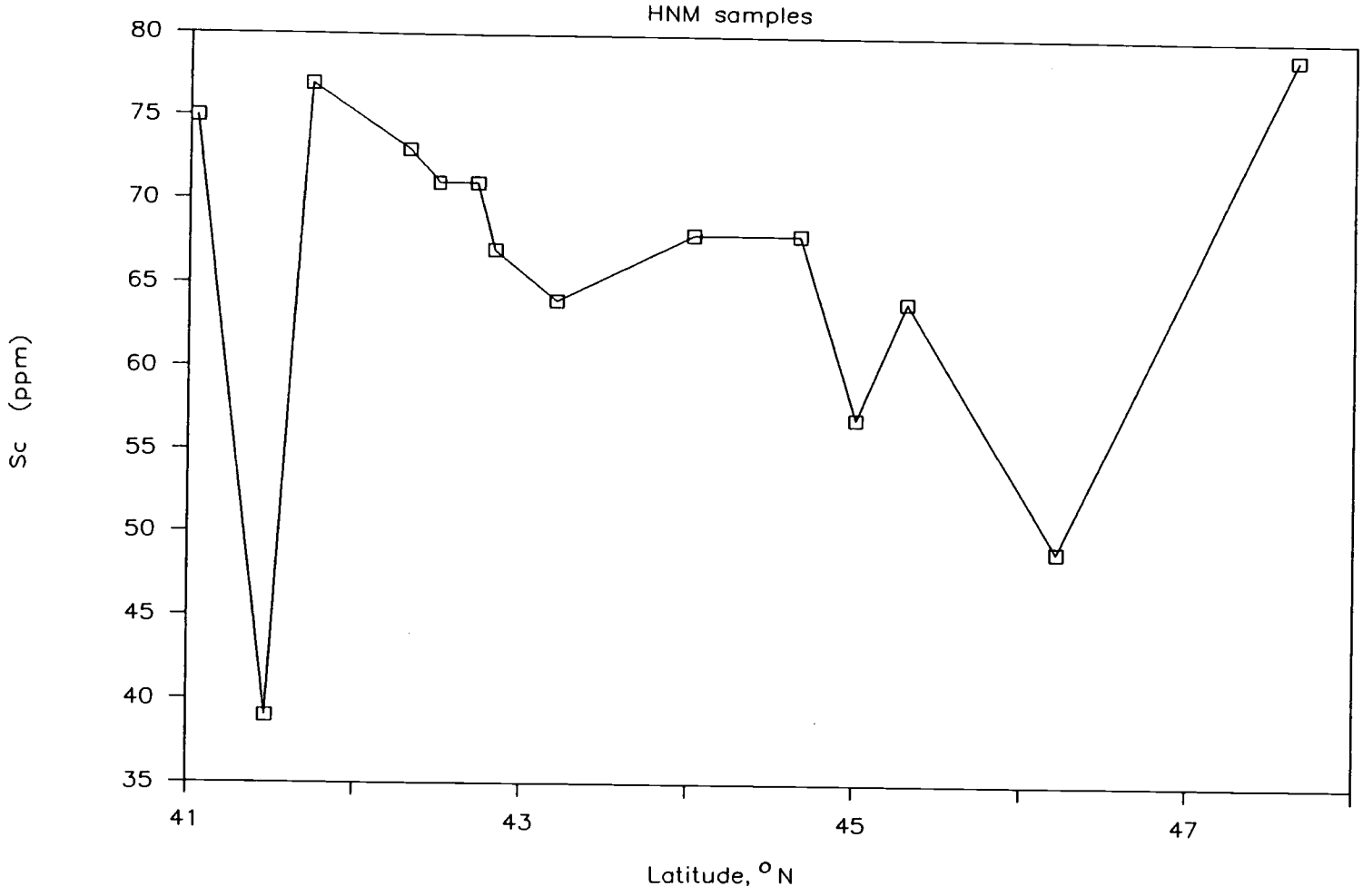

Fig. 17. Scandium concentration versus latitude

Table 13 shows the concentration of lanthanides in the zircon samples. In the lanthanide group the following elements were detected as trace elements: La (< 0.1 - 41 ppm, corrected for contribution from ^{235}U fission), Ce (<1 - 280 ppm; 800 ppm at Moonstone Beach, corrected for ^{235}U fission contribution), Sm (negligible contribution from fission of ^{235}U, < 0.5 - 35 ppm), Eu (1 - 5 ppm), Tb (4 - 13 ppm), Dy (32 - 96 ppm), Yb (<2 - 328 ppm), and Lu (<0.3 - 61 ppm). Lanthanum, Sm, Yb and Lu in the lanthanide group show a very similar abundance trend versus latitude, but the rest of the lanthanides show no particular abundance trend. Figures 18 to 25 show the variation of the lanthanides versus latitude in the HNM samples. Most of the rare earths in the HNM samples followed the trend of the major element, Zr. Also, the heavier rare earths were more abundant in the HNM samples (see Figure 26).

Uranium and Th were also present in the HNM samples as trace elements with a maximum abundance of 426 and 364 ppm, respectively (see Table 14). Figures 27 and 28 show the abundance of U and Th, respectively, as a function of latitude. Figure 29 shows the variation of U as a function of Zr; the two elements seem to a have good linear correlation.

There was a very little amount of Fe (< 1 ppm) in the samples. The abundance of Mn and Na was in the

Table 13

Rare earths concentrations (ppm) in the HNM samples

Sample	La	Ce	Nd	Sm	Eu	Tb	Dy	Yb	Lu
Moonstone	11	800	<78	13	2	5	44	109	26
N. Fern Canyon	6	8	*	10	1	4	32	113	23
Crescent City	<0.1	50	*	5	1	5	59	1	<0.3
Hunters Cove	26	30	*	23	2	8	55	219	44
Nesika	<0.2	148	445	<1	2	6	71	<2	<0.3
Port Orford	28	*	*	26	2	6	75	277	52
Cape Blanco	18	35	*	23	2	10	74	245	48
Sacci	25	*	*	27	1	6	75	283	53
Heceta	29	58	*	34	2	12	96	298	57
Agate	31	67	*	29	1	7	92	308	58
Roads End	28	90	*	30	3	11	78	245	47
Meriweather	41	*	*	35	1	7	80	328	61
Ocean Beach	<0.4	280	498	<1	5	13	91	<2	<0.3
Beach #3	27	*	*	29	2	5	74	279	55

Note: * All concentration due to fission contribution

Underlined data is questionable

TABLE 14

Actinide concentrations (ppm) in the HNM samples

Sample	U	Th
Moonstone	138	82
N. Fern Canyon	121	132
Crescent City	< 0.3	149
Hunters Cove	251	148
Nesika	< 4	364
Port Orford	338	175
Cape Blanco	297	183
Sacci	344	170
Heceta	398	215
Agate	386	219
Roads End	306	172
Meriweather	426	203
Ocean Beach	< 4	227
Beach #3	351	164

Note: Underlined data is questionable

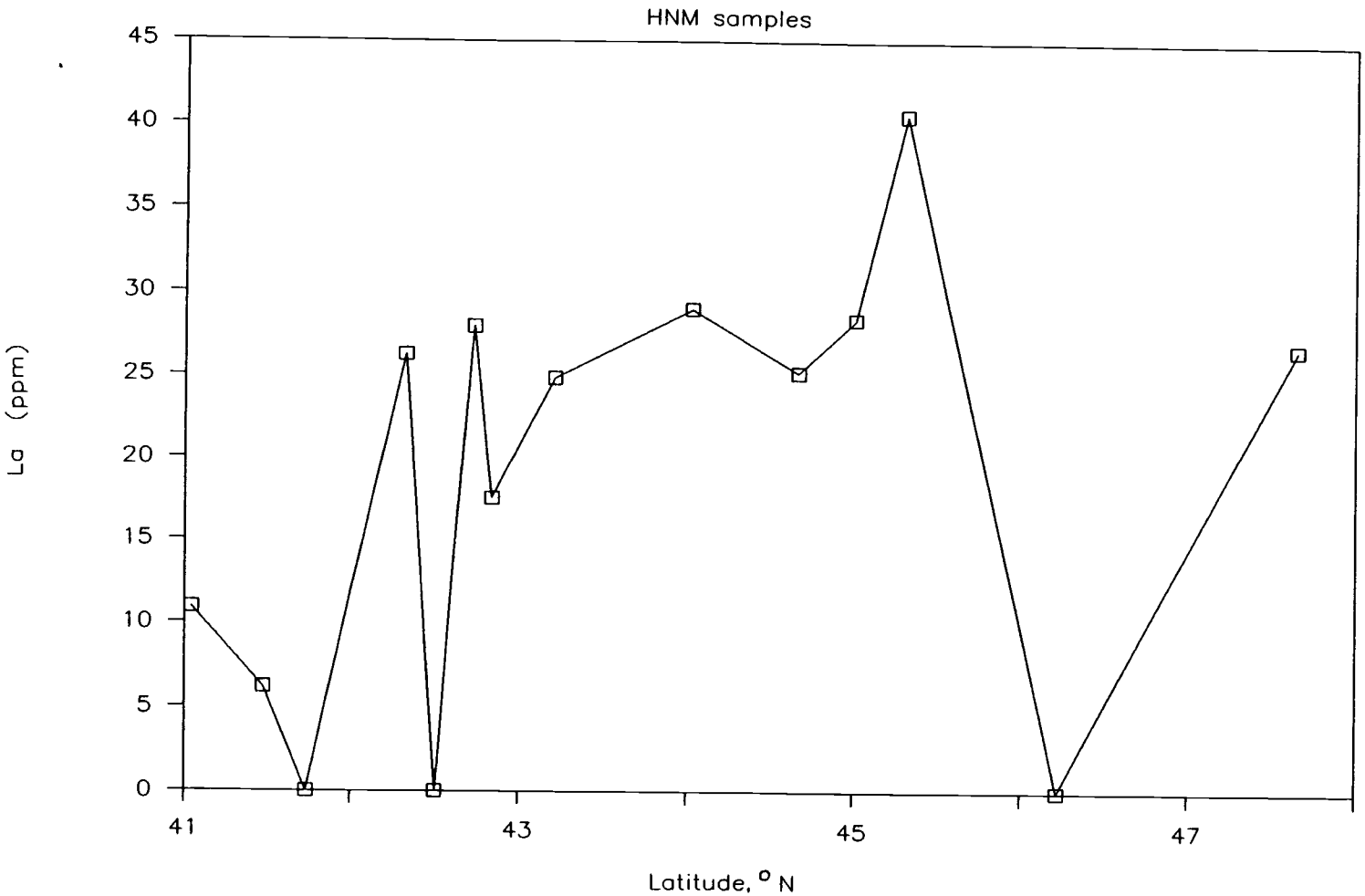

Fig. 18. Lanthanum concentration versus latitude

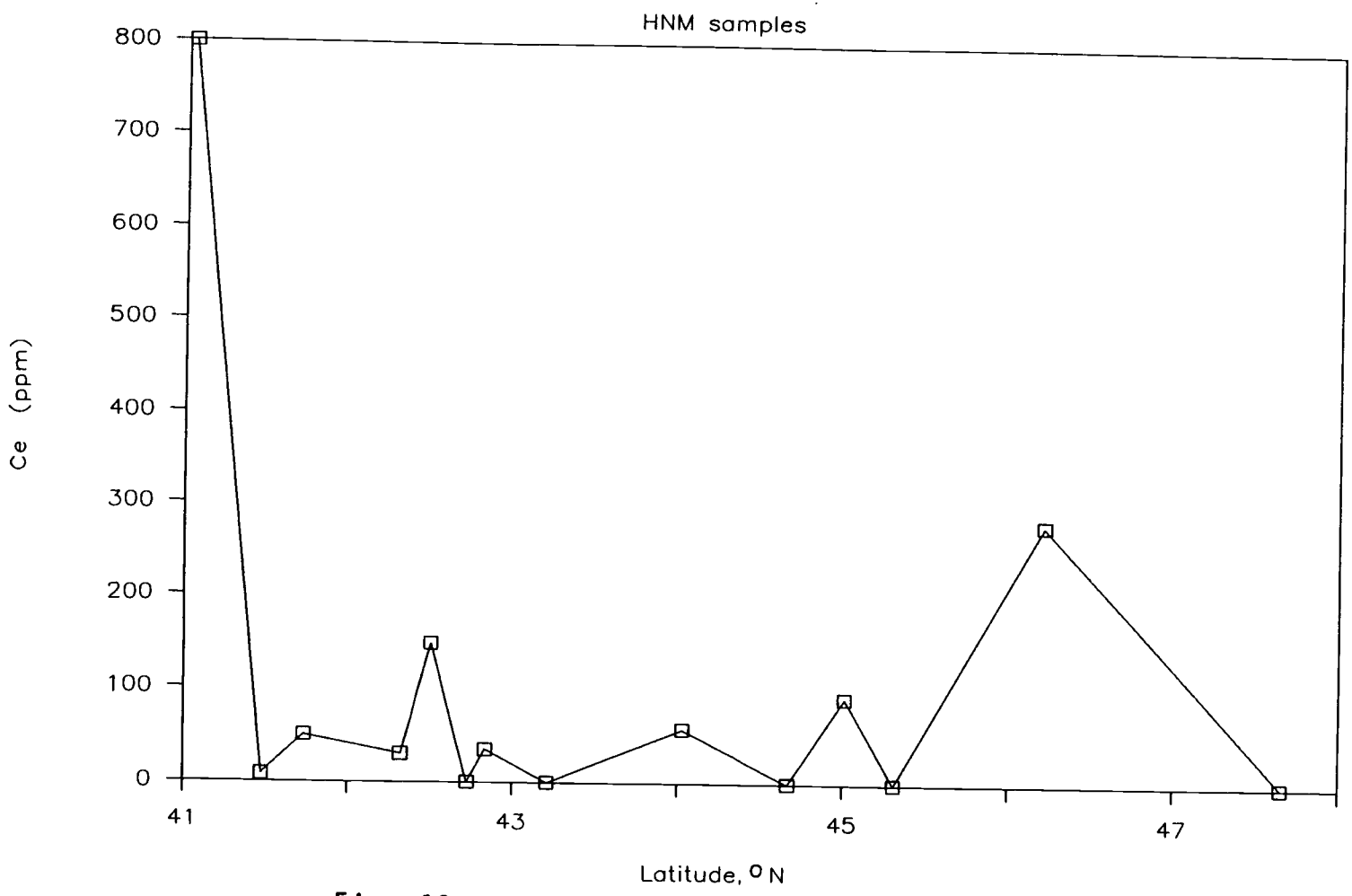

Fig. 19. Cerium concentration versus latitude

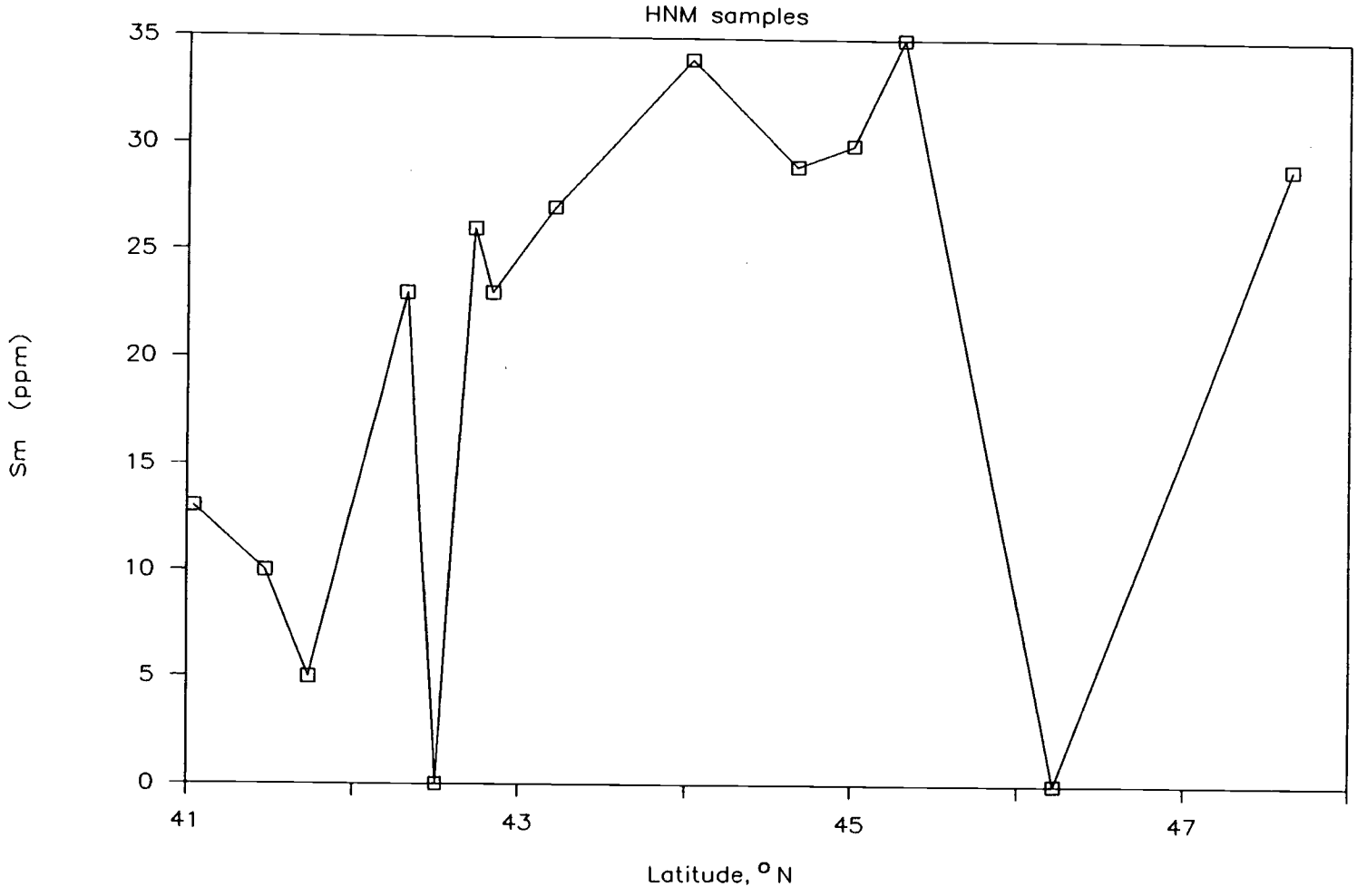

Fig. 20. Samarium concentration versus latitude

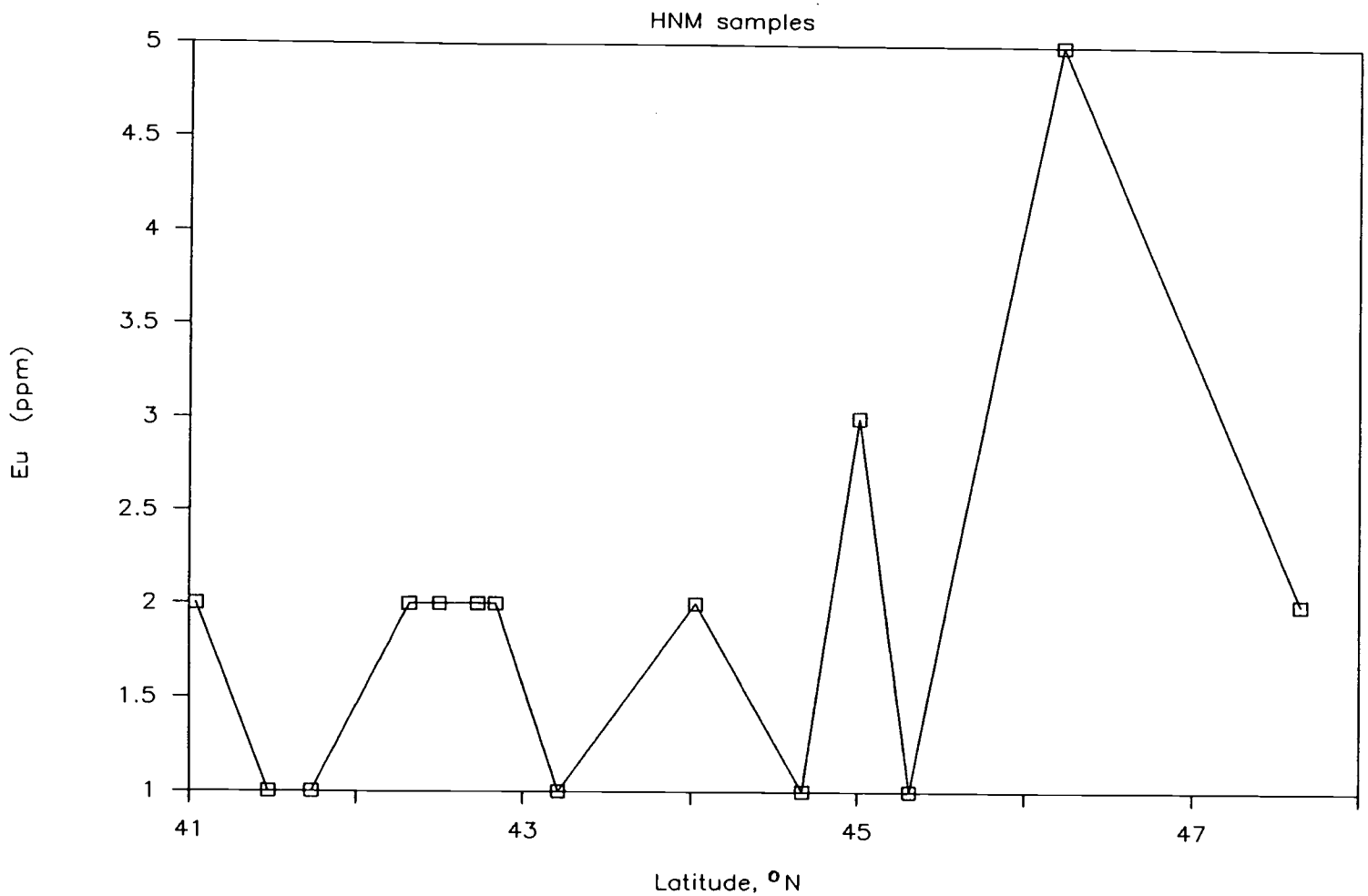

Fig. 21. Europium concentration versus latitude

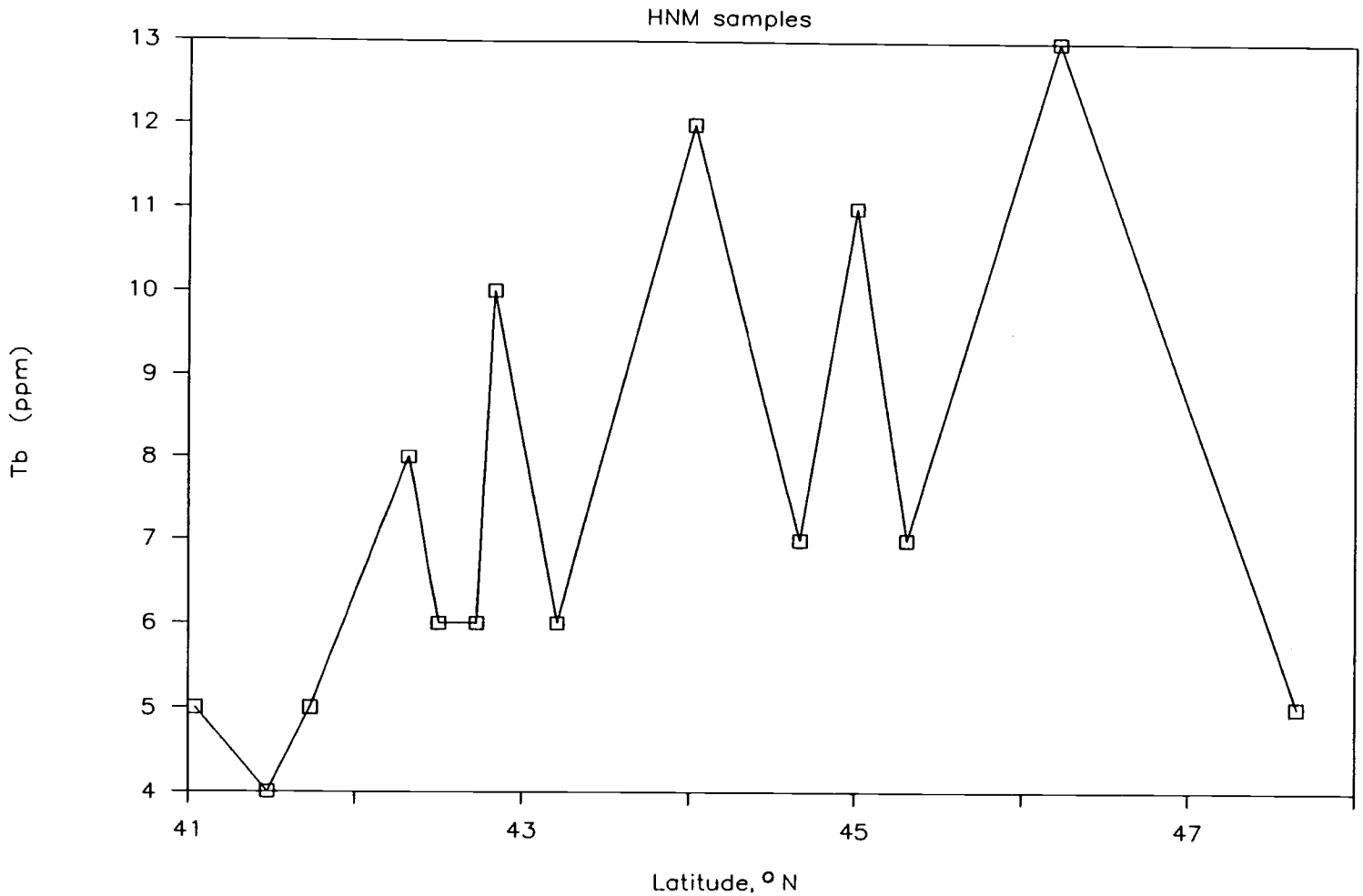

Fig. 22. Terbium concentration versus latitude

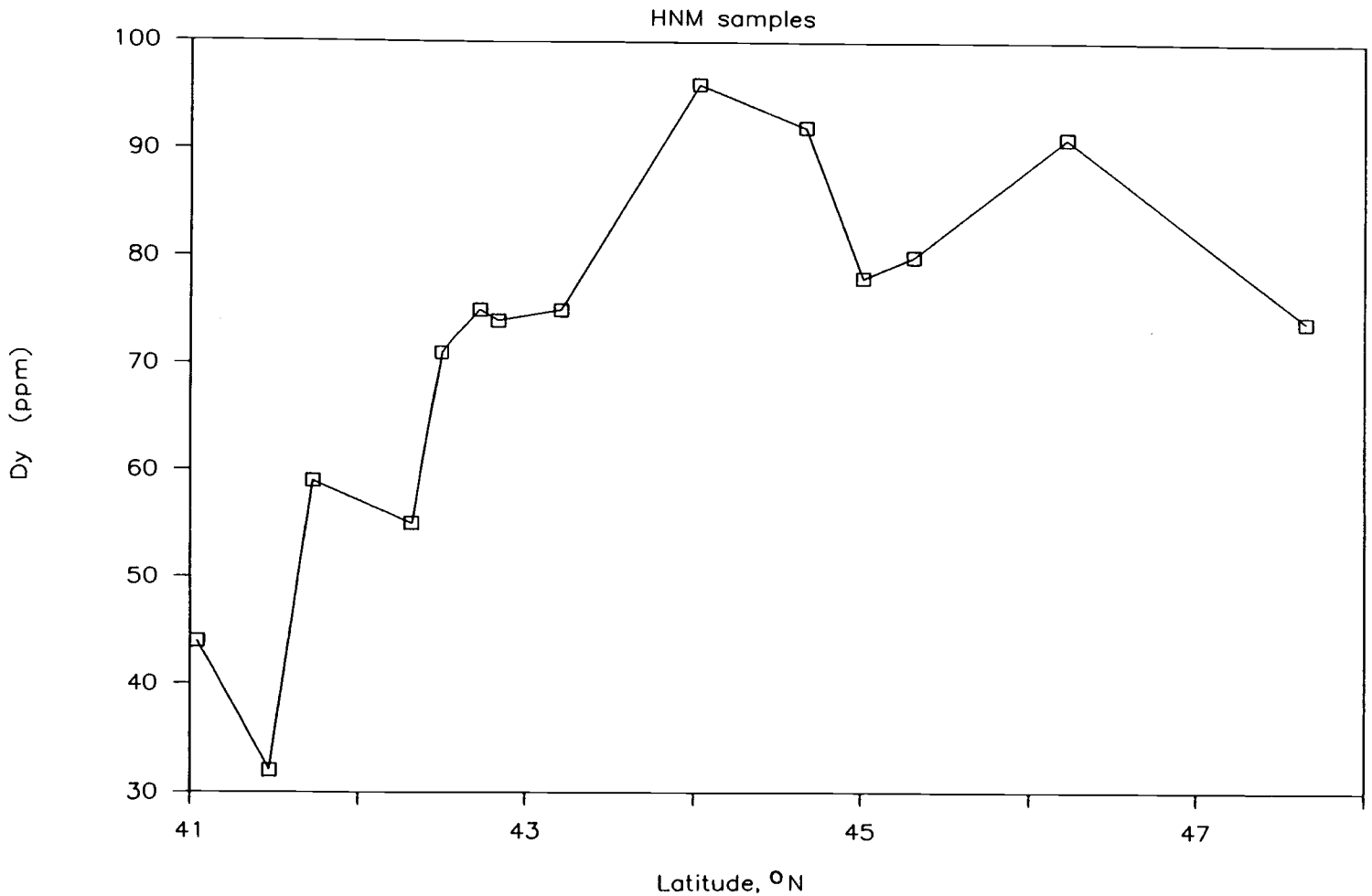

Fig. 23. Dysprosium concentration versus latitude

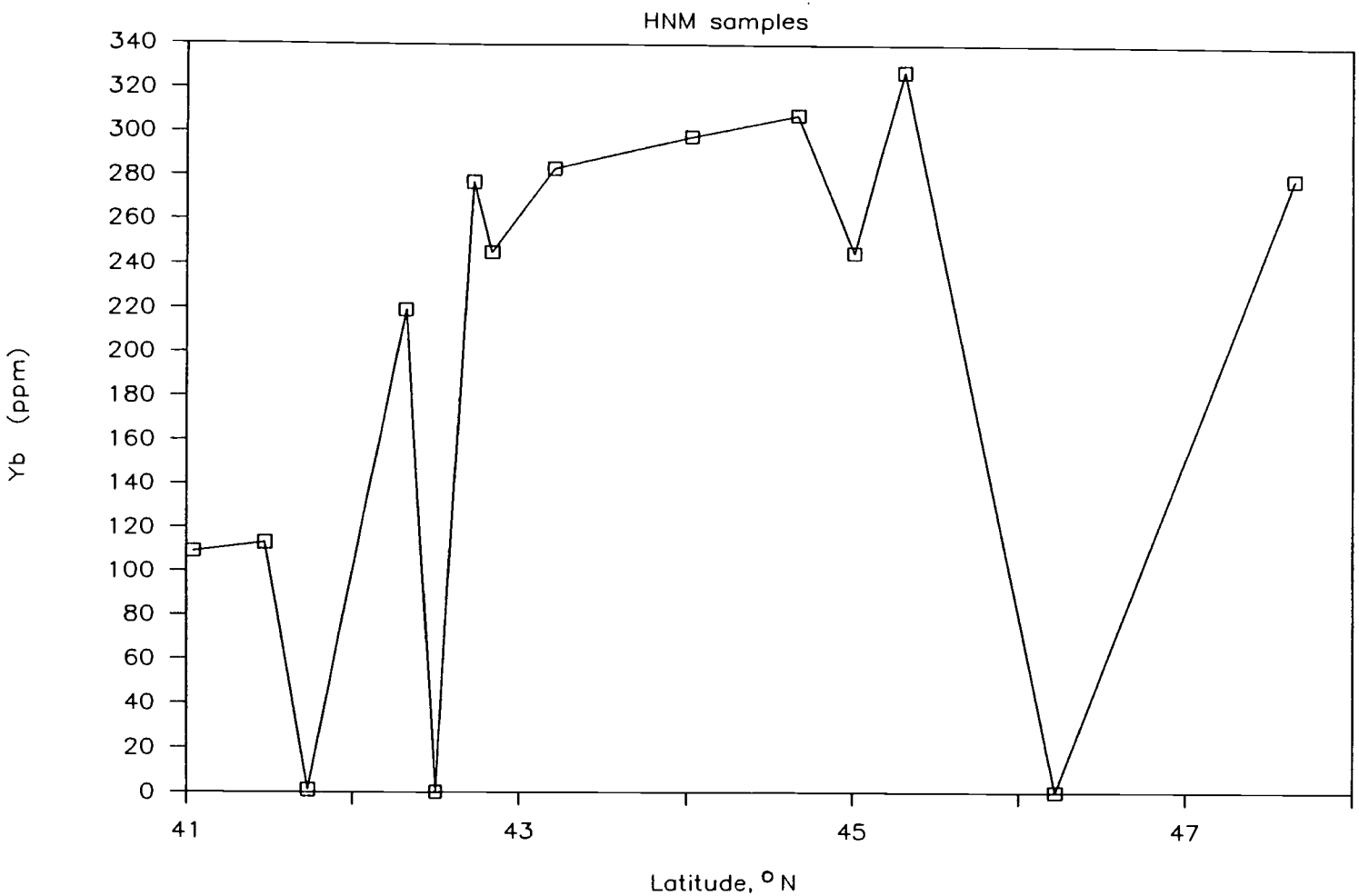

Fig. 24. Ytterbium concentration versus latitude

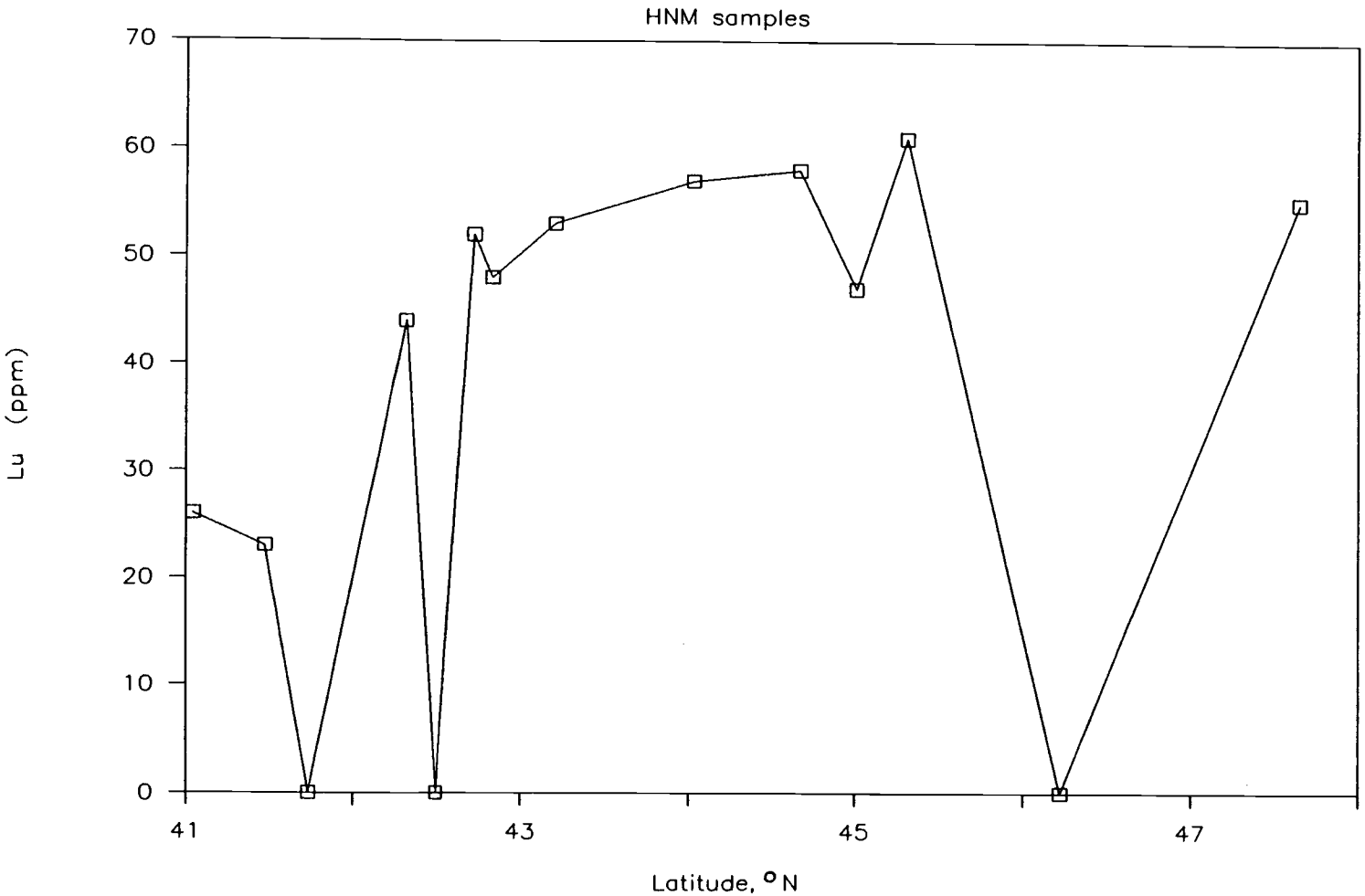

Fig. 25. Lutetium concentration versus latitude

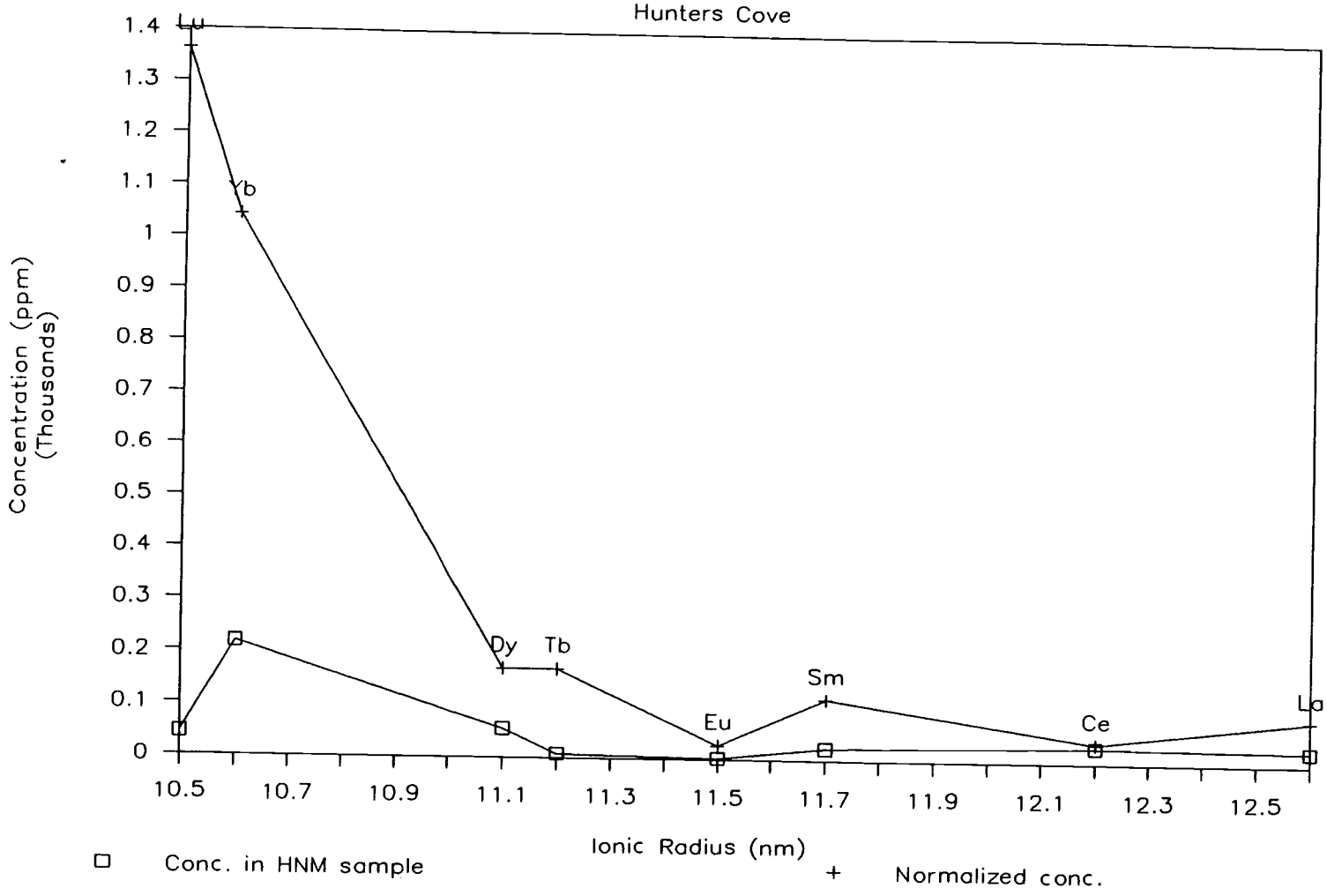

Fig. 26. Rare earths concentration versus ionic radii

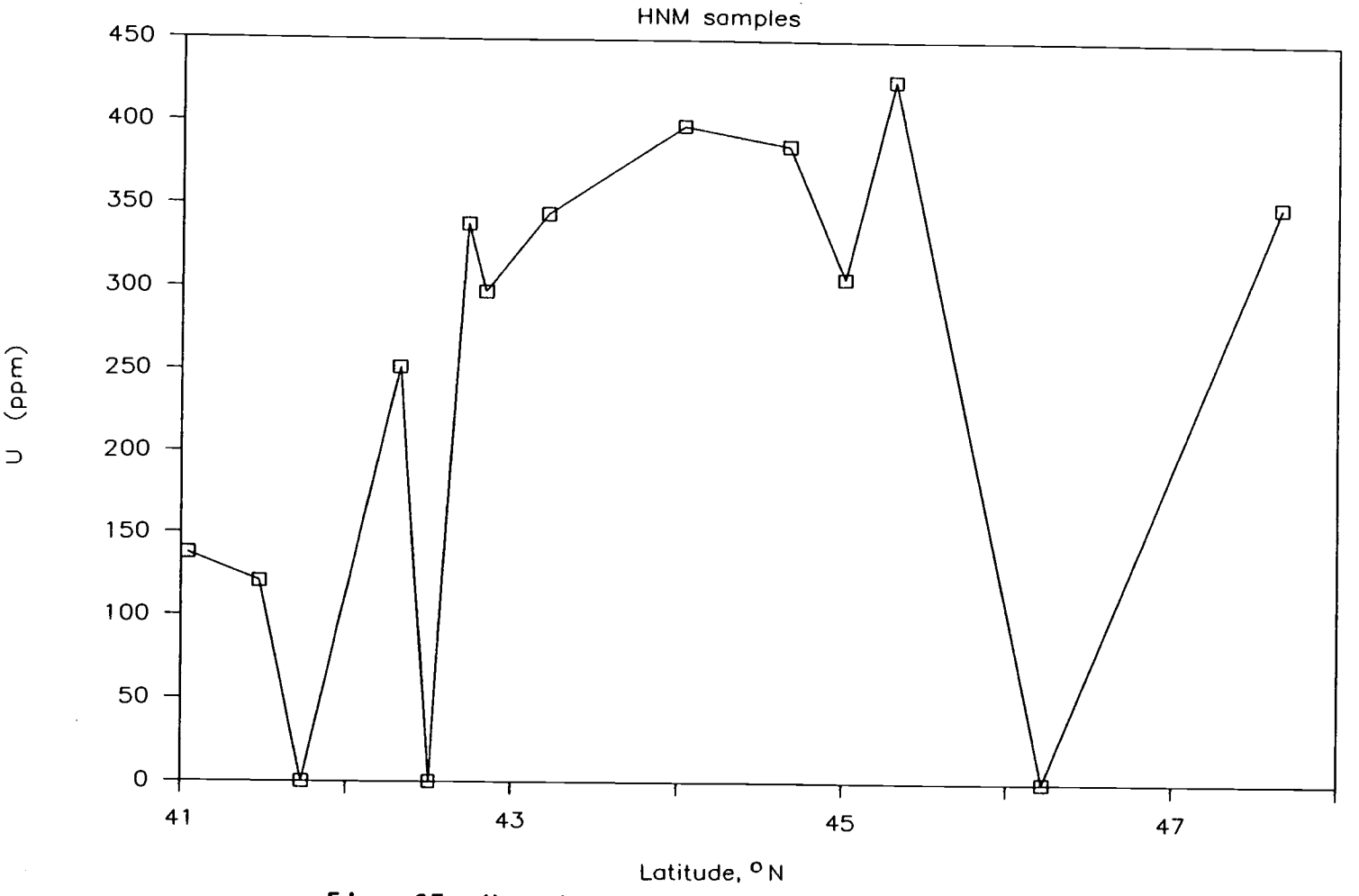

Fig. 27. Uranium concentration versus latitude

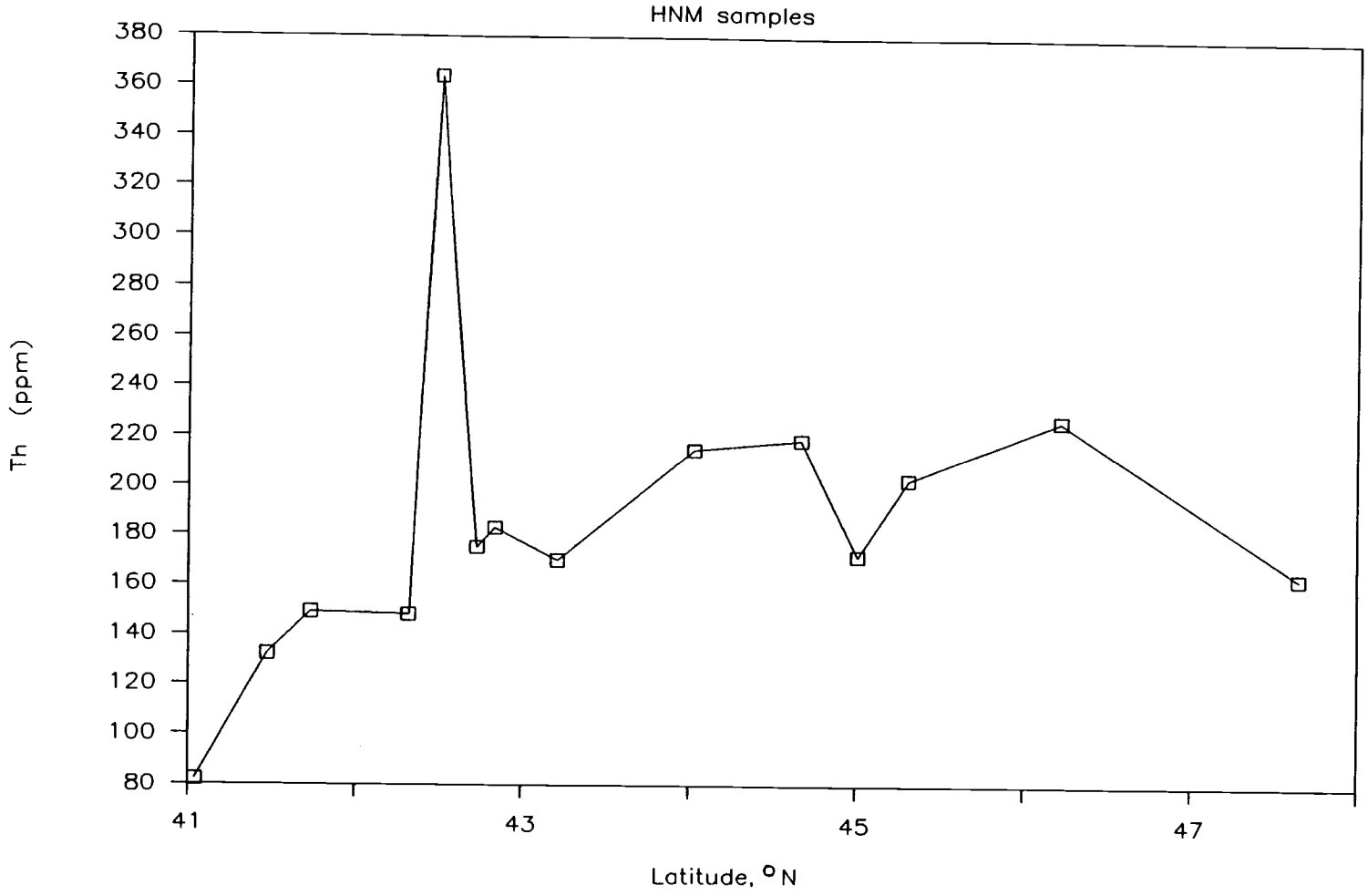

Fig. 28. Thorium concentration versus latitude

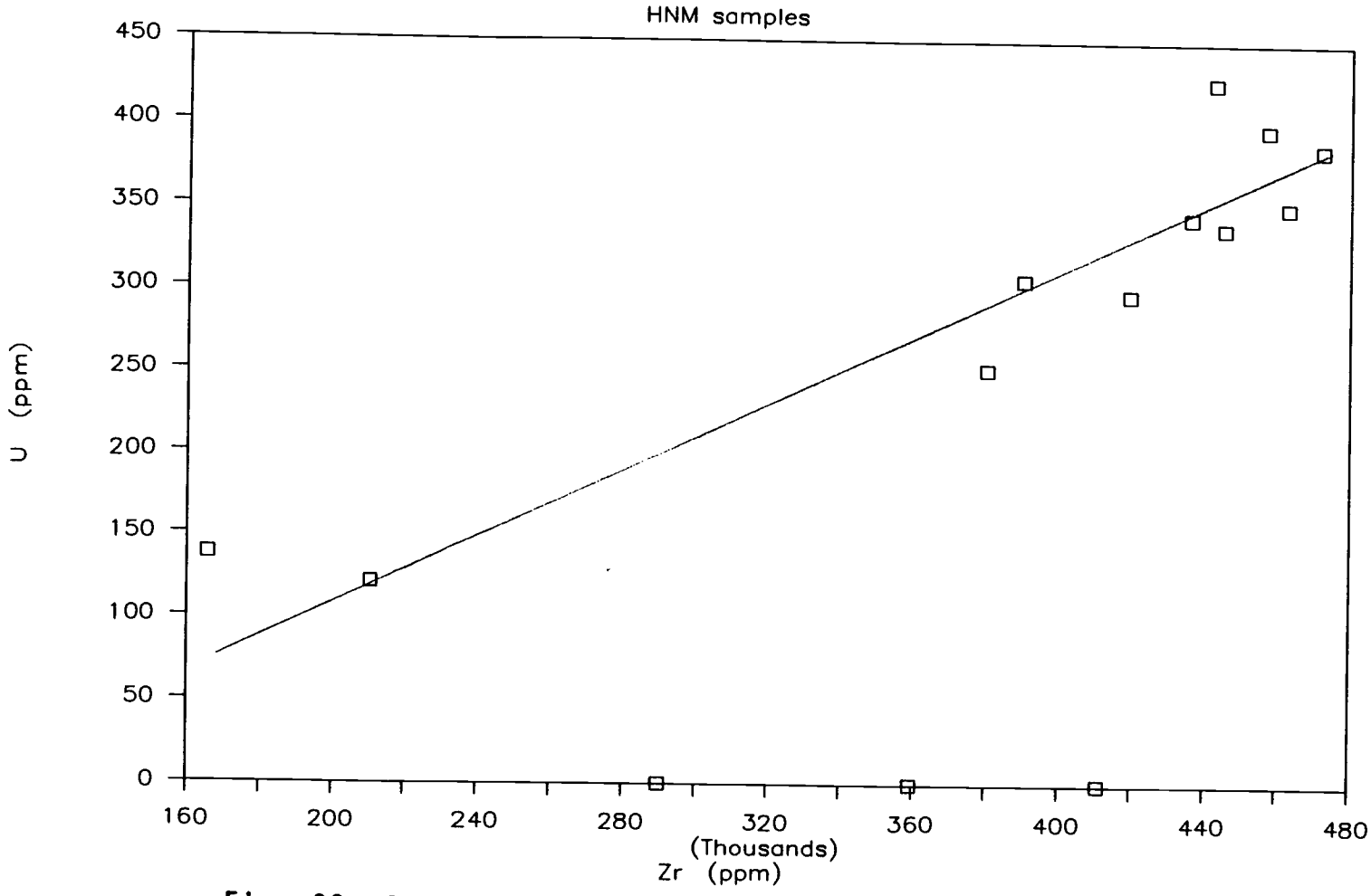

Fig. 29. Correlation between uranium and zirconium abundances

parts per billion range in all of the samples. Potassium was determined for its upper concentration limit only which was less than 1 part per million in any of the samples. Rubidium could only be determined for its upper concentration limit. This was also the case for Co in most of the zircon samples. The samples in which the Co concentration was determined was in the range of 2 - 4 ppm. Table 15 shows the concentrations of these remaining elements in the zircon samples.

TABLE 15

Concentrations (ppm) of other elements in the HNM samples

Sample	Mn	Na	K	Fe	Co	Rb
Moonstone	0.0068	0.01	< 1	0.8	<6	<88
N. Fern Canyon	0.0018	0.02	<0.01	0.4	2	<11
Crescent City	0.0030	0.04	<0.1	0.2	<1	<10
Hunters Cove	0.0040	0.03	<0.1	0.3	4	<18
Nesika	0.0042	0.07	0.02	0.2	4	<26
Port Orford	0.0009	0.01	<0.05	0.2	2	< 7
Cape Blanco	0.0034	0.04	<0.1	<0.2	<2	< 9
Sacci	0.0009	0.01	0.05	<0.1	<1	< 8
Heceta	0.0017	0.02	<0.05	<0.2	<2	<11
Agate	0.0011	0.01	<0.05	<0.1	<2	< 8
Roads End	0.0040	0.05	<0.2	<0.2	<2	<16
Meriweather	0.0021	0.01	<0.05	0.2	<1	< 9
Ocean Beach	0.0064	0.06	<0.2	<0.1	<0.	<35
Beach #3	0.0019	0.01	<0.05	<0.1	1	< 7

5. DISCUSSION

The results in the previous chapter show that the separation techniques employed to separate the zircon from the bulk beach sand worked fairly well because all of the HNM samples (excluding the two southernmost samples with high Ti content) show a very high concentration of zircon (58% - 95%). Based on the physical properties of zircon, a non-magnetic mineral with a specific gravity of 4.67, the method was specifically designed to isolate such a mineral in a sample. This deduction was further strengthened by the near absence of Fe in the samples (< 1 ppm), most of which was removed in the magnetic fraction.

It must be mentioned here that the concentration of Mg could not be determined in most of the samples. The reason for this was that a separate Mg standard was used to calculate the Mg concentration in the samples and to make corrections for the reaction

$$^{27}Al\ (n,p)\ ^{27}Mg$$

It was realized later that the Mg standard had deteriorated during its shelf life, due to photodissociation and precipitation. Hence the results

obtained for Mg were not valid. By the time this was realized, Mg in the samples had decayed to a level where it could no longer be measured. Hence Mg concentrations are not reported for any of the samples.

In the southernmost beaches, such as Moonstone, N. Fern Canyon, Crescent City, and Hunters Cove, there was an appreciable amount of Ti present in addition to Zr. This was observed from the analysis of the HNM samples of the abovementioned beaches, where the concentration of Ti was in the range of 13 - 29%.

There are two possibilities which would explain the presence of Ti in the southernmost HNM samples. One is that the Ti is present in the zircon mineral as a replacement for the Zr atom in the zircon structure, i.e., as $TiSiO_4$. This possibility was supported by the petrographic analysis, since, when the samples were examined under the microscope, they seemed to consist mostly of zircon.

The other possibility is that the Ti is present as rutile. The physical properties of rutile (TiO_2) are very similar to those of zircon. Rutile has a specific gravity in the range of 4.2 - 5.6, and also exists in non-magnetic varieties (low in Fe). Therefore the method employed for the separation of zircon would work equally well for rutile.

When the associated weight percentages of TiO_2 and

$TiSiO_4$ were calculated from the Ti weight percentage in the four southernmost HNM samples, the sum of the rest of the major minerals ($ZrSiO_4$, CaO, and Al_2O_3, [it must be remembered here that Mg, a major element, could not be determined in most of the samples]) plus rutile was approximately 100% within statistical error (see Table 16), whereas if a $TiSiO_4$ structure were considered, the sample weight percentages added up to about 120% (see also Table 16), which does not support the possibility of a Zr atom being replaced by a Ti atom in the silicate structure. Although such a possibility could not be ruled out completely, on a 100% weight basis the $TiSiO_4$ would have to be less than 1% if all the major minerals present were accounted for in the sample. A very high concentration of Ti in zircon has not been previously reported in the literature.

To authenticate the premise that Ti was present as rutile, the HNM sample from N. Fern Canyon was analyzed by the method of X-ray diffraction (XRD) in an independent study. The result of this investigation clearly indicated the presence of rutile. Although XRD study was not carried out on the quantitative basis, it can be assumed that all of the Ti detected is present in the form of rutile. From INAA data analysis, rutile was calculated to be 48% by weight of the zircon sample. Hence it was conclusively established that Ti

TABLE 16

Weight percentages of the Ti and Zr minerals in the HNM samples

Sample	$ZrSiO_4$	$TiSiO_4$	Total*	TiO_2	Total**
Moonstone	33.25	82.46	124.	47.12	88.
N. Fern Canyon	42.32	83.93	128.	47.96	94.
Crescent City	72.20	37.64	113.	21.65	97.
Hunters Cove	76.40	45.40	128.	25.94	108.
Nesika	82.60	18.63	104.	10.64	96.
Port Orford	89.50	8.85	101.	5.05	97.
Cape Blanco	84.30	18.25	108.	10.43	100.
Sacci	87.60	7.48	99.	4.27	94.
Heceta	91.80	15.06	109.	8.61	103.
Agate	94.85	4.56	102.	2.60	100.
Roads End	78.40	8.64	101.	4.94	98.
Meriweather	88.90	7.18	98.	4.10	95.
Ocean Beach	58.20	23.74	96.	13.58	86.
Beach #3	92.97	6.37	102.	3.64	99.

Total*: Total of major elements with Ti as $TiSiO_4$

Total**: Total of major elements with Ti as TiO_2

TABLE 16 (continued)

Note:

TiO_2 wt% = 1.67 x Ti wt%

$TiSiO_4$ wt% = 2.92 x Ti wt%

$ZrSiO_4$ wt% = 2.01 x Zr wt%

Al_2O_3 wt% = 1.89 x Al wt%

CaO wt% = 1.40 x Ca wt%

$BaSO_4$ wt% = 1.70 x Ba wt%

HfO_2 wt% = 1.18 x Hf wt%

was present in the southernmost samples in the form of rutile as evidenced by the calculational data presented in Table 16, and the result of X-ray diffraction method.

From the data analysis conducted on the magnetic portions of the samples [16] from the same southernmost beaches (Moonstone, N. Fern Canyon, Crescent City, and Hunters Cove), the concentration of Ti present was determined to be in the range of 1 - 10% of the magnetic fraction of the bulk sample. Thus the presence of Ti on the southernmost beaches was indicated in earlier research, although in the magnetic portion of the samples. In those samples the Ti was found in the mineral ilmenite, which is a magnetic mineral. In this project the samples were the non-magnetic portions of the same beach samples. Hence the presence of Ti in the zircon samples indicates a somewhat higher total concentration of Ti in the beach sands of northern California and southern Oregon than previously established, although the concentration of Ti in the HNM fraction may not be an appreciable fraction of the bulk sand. Also, since the results of this study and previous work [16] indicate that there are two minerals of Ti (rutile and ilmenite) present on the beaches, this could possibly imply two different sources of Ti minerals for these beaches. A regression analysis (see Appendix C) was employed to calculate the linear

correlation coefficient r between each pair of elements observed in the HNM samples. For the two elements Ti and Zr, the value of r was -0.91, which is very close to -1.00, the negative sign indicating an inverse correlation.

In addition to Ti, Zr is the other major element of interest which was present in appreciable concentrations (16.6 - 47.2% by weight of HNM fraction) in the HNM samples. It is observed from the data that the Zr concentration as a function of latitude depends on the relative abundance of other major elements present in the sample. The high concentration of Ti in the HNM samples in the southernmost beaches fingerprints those beaches as being somewhat unique in their composition. Since there was only one sample from the Washington beaches, it cannot be stated conclusively whether this trend is followed further north.

When the HNM samples are divided into two groups (one group consisting of the eight southernmost samples, and the other group consisting of the six northernmost samples), and Zr/Hf ratio and its standard deviation come out to be very close in numerical value (see Table 11). Looking at the geological locations of the bulk samples, it can be said that the sand in the first group was formed by the erosion of the Klamath Mountains region, and that in the second group by the erosion of

the Coast Range and Columbia River basalt. Similar Zr/Hf ratios for the two groups imply that the zircon in the sands probably originated from very similar sources.

It may be mentioned here that all of the samples were collected from south side of headlands, i.e., part of the land that juts out into the ocean.

The heavy non-magnetic fraction consisted mostly of mineral zircon (58 - 95% by weight of the HNM fraction). The concentration of zircon peaked at Agate Beach, which is at a latitude of 44.67°N (see Table 17). At this location the zircon weight percentage, calculated as the percent of the heavy fraction (≥ 3.0 specific gravity) of the bulk sample, is 7.6%. Agate Beach was followed in zircon concentration by Port Orford at 6.46%. A similar calculation for Sacci and Meriweather beaches gave the percentage of zircon as 4.56% and 4.65%, respectively. For Cape Blanco the zircon percentage was 2.27%. For the rest of the samples the zircon abundance was less than 1% of the heavy fraction (see Table 17).

For industrial uses, zircon is obtained as a by-product of the Ti minerals, which is the main reason for mining the beaches. The sands which are considered to be economically minable contain 4% by weight of the heavy minerals. The heavy mineral fraction has 55% by weight of the Ti minerals and has >10% zircon; the rare

Table 17

Zircon content of the HNM and heavy fractions

Sample	Zircon in HNM (%)	HNM mass (g)	Heavy sample (g)	%Zircon heavy
Moonstone	33.25	0.0082	32.66	0.01
N. Fern Canyon	42.32	0.3765	49.50	0.32
Crescent City	72.20	0.1626	62.17	0.19
Hunters Cove	76.40	0.0520	7.57	0.52
Nesika	82.60	0.0279	18.19	0.13
Port Orford	89.50	0.3751	5.15	6.52
Cape Blanco	84.30	0.0825	3.04	2.29
Sacci	87.60	0.4867	9.35	4.56
Heceta	91.80	0.0677	6.70	0.93
Agate	94.85	0.6664	8.33	7.59
Roads End	78.40	0.0515	13.73	0.29
Meriweather	88.90	0.3403	6.50	4.65
Ocean Beach	58.20	0.0270	5.67	0.28
Beach #3	92.97	0.4471	51.1	0.81

Note: Masses of the heavy fraction is rounded-off to 2 significant numbers

earth content is about 1% of the heavy fraction. A marketable zircon concentrate has 99% zircon. A standard grade zircon contains 65% zirconia (ZrO_2), while the premium grade zircon concentrate has 66% zirconia [23].

Based on the above information, it is deduced that at present mining of Oregon beaches would not be economically feasible unless the heavy mineral content of the bulk samples equals or exceeds 4%. Zircon is a widely abundant mineral worldwide and at present its demand and supply are well-balanced. Projection and forecast for U.S. Zr demand by the year 2000 (see Table 18) is well exceeded by the available Zr, estimated as present in reserve and reserve base (see Table 19). However if this balance is interrupted, it may become economically desirable to mine zircon from the Pacific coast beaches or, more likely, from the offshore placer deposits.

The same regression routine as mentioned previously gave a linear correlation coefficient for Zr and Hf of +0.99, and +0.95 for Ti and V. The correlation coefficient was -0.91 for Ti and Zr; hence it can be said a strong correlation exists between the four abovementioned elements. Iron also had a strong negative correlation with the major element Zr (-0.89).

Some of the lanthanides showed some correlation

TABLE 18

Projection and Forecast for U.S. zirconium demand by end use - 2000

(Short tons of zirconium content)

End use	1983	2000
Non-metal:		
Iron and steel foundries	24000	48000
Refractory	14000	35000
Ceramics and glass	3000	12000
Abrasives	W	7000
Chemicals	400	3000
Others	1600	6000
Metal:		
Nuclear reactors	1600	1000
Fabricated metal products	100	200
Photography	50	70
Steel and other alloys	2700	3800
Grand total (rounded)	47000	116000

Note: W - withheld to avoid disclosing company propriety data

TABLE 19

World zirconium reserves and reserve base

(Thousand short tons of zirconium content)

Country	Reserve	Reserve base
U.S.A.	4000	8000
Canada	-	1000
Brazil	250	2150
U.S.S.R.	3000	5000
Madagascar	100	200
Sierra Leone	500	2000
South Africa	3400	12100
China	400	1000
India	1800	3000
Malaysia and Thailand	100	200
Sri Lanka	1000	1500
Australia	8700	14900
World total (rounded)	23000	51000

Note: Reserve base = Currently economic + marginally economic + subeconomic

with the major element Zr, such as La (0.82), Sm (0.75), Yb (0.74), Lu (0.96), and Dy (0.72). Uranium also followed the trend of the major element Zr ($r = 0.94$).

A strong linear regression between two elements implies that if some data are acquired for a similar sample, giving only the concentration of one of elements, rough estimates can be made for the other element. This logic can be extended to more than two elements.

One of the major elements, Al, has a strong linear correlation with the trace elements Co and Zn (0.92 and -0.82, respectively). Similarly another major element Ca correlates strongly with Mn, Fe, Co, and Eu. Hence the presence of one element would serve as an indicator for the other elements.

There were certain anomalies associated with the rare earths present in the HNM samples. For example, although the concentration of Sc and Dy in the HNM samples from Crescent City, Nesika, and Ocean Beach were typically expected values (see Table 12), the concentrations obtained for Ce, Nd, and Lu were not as expected. The concentration of U at the abovementioned beaches was also questionable. These anomalies could be attributed to the fact that the radioisotopes of Ce, Nd, Lu, and U all have photopeaks of low energies (146 keV, 91 keV, 208 keV, [106, 278] keV, respectively, see Table

9), which fall into regions where the background is high. The Compton continuum is also high at low energies. Another reason could be interference from other photopeaks, for example, the second photopeak of Nd at 531 keV can have interference from the 511 keV annihilation peak. Also the masses of the samples from Nesika and Ocean Beach were very small (~ 20 mg), so that the number of counts in the photopeaks were low, resulting in larger errors. The mass of the sample from Crescent City was >150 mg, so counting statistics is not a concern in this case. But in this case the Compton continuum would be higher due to the greater activity of the sample.

Most of the rare earth elements present in the HNM samples followed the trend of the major element Zr in the samples. When the concentration of the rare earths in the HNM sample from Hunters Cove was normalized to the concentration of the rare earths in the earth's mantle, a smooth curve was obtained (see Figure 26). This gives confidence in the rare earth results obtained because these results agree with typical values obtained in geological samples (24). This behavior was generally followed by the lanthanides in all samples, even in the ones which had somewhat anomalous results.

It can be observed from Figure 26 that Eu appears to be depleted in the samples. The reason for this is

that the beach sands are formed by the erosion of granites, which have their origin in the plagioclase (commonest rock forming minerals). The plagioclase has an affinity for Eu^{+2}; hence Eu was depleted in the granite, which later formed the sands.

Figure 26 also indicates that the HNM samples are richer in the heavier rare earths, since the ionic radius reduces for the heavier element in the lanthanide series, thereby making it easier for the heavier lanthanide ions to fit into the zircon structure.

6. SUMMARY

The aim of this project was to analyze the HNM fraction of the beach samples from the Pacific Northwest coast for their elemental content. Samples from fifteen beaches were selected for this purpose. Zircon is a non-magnetic mineral of Zr with a specific gravity of 4.67. A separation scheme was devised to separate zircon from the bulk beach sample which contains several minerals of various magnetic susceptibilities and specific gravities. The separation culminated in a sample fraction which consisted mostly of zircon. This fraction, termed the HNM sample, was analyzed for its elemental content.

The HNM samples were analyzed by the method of instrumental neutron activation analysis (INAA). A sequential scheme was carried out to detect the elements present in the samples. Sequential analysis of the samples was based on the half lives and required appropriate decay periods for the radioisotopes which were most likely to be found in a geological sample.

From the analysis of the data obtained by the above method, it was found that Zr was present as a major element in the samples. The weight percent of zircon in the HNM samples was in the range of 58 - 95%. In the

samples from the southernmost beaches (northern California), there was an appreciable amount of Ti present along with Zr. The Ti mineral present in the samples is expected to have similar physical properties to zircon because it was separated out of the bulk sample through the same rigorous separation scheme as zircon. The zircon and the Ti mineral had an inverse correlation in which the increase in concentration of one element was associated with a decrease in concentration of the other element. Although the presence of a Ti mineral such as rutile was not indicated by petrographic analysis, neither could the presence of Ti in the zircon structure itself be verified by weight percentage estimation of all the major elements present in the samples. This peculiarity observed in some of the samples was solved by the results of an independent investigation by X-ray diffraction analysis, which indubitably identified the titanium mineral as rutile.

The other elements which were present in the samples as either major or minor elements were Ca, Mg, Ba, and Hf. Hafnium followed the geological trend of Zr, as did U. Vanadium, which was a trace element in the samples, followed the geological trend of the major element Ti.

Lanthanides were present in the samples as trace

elements and generally correlated well with Zr. The normalized concentration (with respect to the abundance in the earth's mantle) of lanthanides plotted as a function of their ionic radii resulted in a smooth curve, which was a further verification of the fact that the values determined for the concentration of rare earth elements in the zircon samples were typically observed values in a geological sample.

Zircon is a widely available mineral, and at present the Oregon beaches could only be considered as a reserve base for Zr.

REFERENCES

1. U.S. Congress, Office of Technology Assessment, "Marine Minerals: Exploring Our New Ocean Frontier," OTA-O-342 (Washington, DC: U.S. Government Printing Office, July 1987).

2. Peterson, C.D., Komar, P.D., Scheidegger, K.F., "Distribution, Geology, and Origin of Heavy Mineral Placer Deposits on Oregon Beaches," Journal of Sedimentary Petrology, 56, No. 1, p. 67-77 (1986).

3. Wogman, N.A., "In-situ X-ray Fluorescence and Californium-252 Neutron Activation Analysis for Marine and Terrestrial Mineral Exploration," Proceedings of IAEA Symposium on Nuclear Techniques and Mineral Resources, IAEA-SM-216156, p. 447-463 (1977).

4. Noakes, J.E., Harding, J.L., "New Techniques in Seafloor Mineral Exploration," MTS Journal 5, p. 41-44 (1971).

5. Noakes, J.E., Harding, J.L., "Nuclear Techniques for Seafloor Mineral Exploration," Oceanology International Exhibition and Conference, Brighton, England, p. 0182 (1982).

6. Senftle, F.E., Duffy, D., Wiggins, P.F., "Mineral Exploration on the Ocean Floor by In-situ Neutron Absorption using a Californium-252 (^{252}Cf)

Source," MTS Journal 3(5), p. 9 (1969).

7. Senftle, F.E., Tanner A.B., Philbin, P.W., Noakes, J.E., Spalding, J.E., Harding, J.L, "In-situ Capture Gamma ray Analyses for Seabed Exploration," Proceedings of a Panel on Nuclear Techniques in Geochemistry and Geophysics, Vienna, p. 75-91 (1974).

8. Moxham, R.M., Tanner, A.B., Senftle, F.E., "In-situ Neutron Activation Analysis of Bottom Sediments, Anacostia River, Washington D.C.," MTS Journal 11, p. 14 (1975).

9. Weast, R.C., Editor-in-chief, CRC Handbook of Chemistry and Physics, 64th edition, p. B-40 (1983).

10. Hess, H.D., "Hafnium content of Domestic and Foreign Zirconium Materials," United States Department of Interior, US Bureau of Mines, p. 3-8 (1961).

11. Bates, R.L., Jackson, J.A., editors, Dictionary of Geological Terms, 3rd Edition, prepared by American Geological Institute (1984).

12. Phillips, W.R. and Griffen, D., Optical Mineralogy The Nonopaque Minerals, W. H. Freeman & Company, San Francisco, p. 677 (1981).

13. Hurlbut, Jr., C.S., Klein, C., Manual of Mineralogy, 19th edition, John Wiley & Sons, New York (1983).

14. Libbey, F.W., State Department of Geology and Mineral Industries, Private communication to George W.

Gleeson, January 25, 1945.

15. de Soete, D., Gybels, R., Hoste, J., Neutron Activation Analysis, Wiley Interscience, p. 65 (1972).

16. Peterson, C.D., Binney, S.E., "Nature and Compositional Variation of Coastal Placer Deposits in the Pacific Northwest Region, USA," submitted to Marine Mining (1988).

17. Knoll, G.F., Radiation Detection and Measurement, John Wiley & Sons, New York, NY, p. 313-316 (1979).

18. Hevesy, G. and Levi, H., "The Use of Neutrons in Analytical Chemistry," Math. Fys. Med. 14(5), p. 34 (1936).

19. Gladney, E.S., "Elemental Concentration in NBS Biological and Environmental Standard Reference Materials," Analytica Chemica Acta 118, p. 385 (1980).

20. Gladney, E.S., Burns, C.E., Roelandts, I., "1982 Compilation of Elemental Concentration in Eleven United States Geological Survey Rock Standards", Geostandards Newsletter, 7(1), p. 3 (1983).

21. Laul, J.A., "Neutron Activation Analysis of Geological Materials," Atomic Energy Review, 17(3), p. 603-695 (1979).

22. Pehl, R.H., "Germanium Gamma Ray Detectors," Physics Today, 14(6), p. 50 (1977).

23. Adams, W.T., "Mineral Facts and Problems,"

Bureau of Mines Bulletin 675, p. 941-954 (1985).

24. Laul, J.C., Keays, R.R., Ganapathy, R., Anders, E., Morgan, J.W., "Trace Elements in Rocks," Geochemica Cosmochemica Acta, 36, p. 329 (1972).

25. Robinson, K., Gibbs, G.V., Ribbe, P.H., "Structure and Metamictization of Zircon," American Mineral, 56, p. 782-790 (1971).

26. Walker, F.W., Miller, D.G., Feiner, F., "Chart of Nuclides," General Electric Company (1984).

APPENDICES

APPENDIX A

PROPERTIES OF ZIRCON AND ZIRCONIUM [25]

TABLE A-1

Geological properties of zircon

Crystal system:	Tetragonal
Lattice:	I
Cell dimensions:	a = 6.604, c = 5.979
Content:	Z = 4
Cleavage:	{110}, indistinct
Hardness:	7.5
Density:	4.6 - 4.7 when crystalline, decreasing to 3.9 when metamict.
Color:	Usually brown to reddish brown, but can be colorless, gray, green or violet; the transparent variety used as gemstones are produced by heat treatment of natural zircon.
Chemistry:	In zircon some of the Zr is always replaced by Hf (generally about 1%, but up to 4% has been recorded). Part of Zr can also be replaced by rare earths, coupled with replacement of zirconium by phosphorus. Zircon is frequently radioactive by the presence of Th and U replacing Zr in the structure; as a result of radiation damage from these radioactive elements, these zircon are often metamict.
Diagnostic features:	Habit, hardness, color, and density are useful distinguishing

features of zircon.

Occurrence: Zircon is a common accessory mineral of igneous rocks and pegmatites of granites, syenite, and nepheline syenite families. The presence of uranium and thorium makes it a useful mineral for age determination of such rocks. Because zircon is resistent to chemical disintegration, it appears as a detrital mineral in river and beach sands.

Production and uses: Zircon is the principal source of zirconium and hafnium in industry. It is extracted from sands.

TABLE A-2

Chemical and nuclear properties of zirconium [26]

Chemical symbol:	Zr
Preferred valence:	+4
Atomic number:	40
Atomic mass:	91.22 a.m.u.
Boiling point:	4682 K
Melting point:	2125 K
Density:	6.49 g/cm^3 (at 300 K)
Stable isotopes: (abundance)	^{90}Zr (51.45%), ^{91}Zr (11.27%), ^{92}Zr (17.17%), ^{94}Zr (17.33%), ^{96}Zr (2.78%)
Neutron absorption cross section:	0.18 barns.

APPENDIX B

EQUATION FOR INAA

The basic equation for NAA for an element x is as follows:

$$D_x = \frac{NWF\sigma\phi}{M} (1-e^{-\lambda_x T}) e^{(-\lambda_x t)}$$

$$A_x = KD_x$$

where

D_x = disintegrations/s of a radionuclide x at time t after the end of irradiation

A_x = activity (counts/s) of a radionuclide x at time t

K = proportionality constant - including detection efficiency and nuclear decay scheme of x

N = Avogadro's number, 6.02×10^{23} atoms/mole

W = mass of an element x irradiated, in grams

F = fractional isotopic abundance of target element

M = atomic weight of the element x

σ = nuclear reaction cross-section in cm^2

ϕ = flux of neutrons ($cm^{-2}.s^{-1}$)

λ = decay constant of the radionuclide

T = irradiation time

t = decay time after end of irradiation

The neutron activation analysis equation by the

comparative method is obtained from the above equation by calculating activity for a single element in the standard and the sample:

$$\frac{\text{mass of element x in the sample}}{\text{mass of element x in standard}} = \frac{A_x \text{ in sample } e^{+\lambda t_x}}{A_x \text{ in standard } e^{+\lambda t_s}} \quad \text{(B-1)}$$

where

t_x = decay time after the end of irradiation in sample

t_s = decay time after the end of irradiation in standard

A_x = measured activity of the radionuclide x at start of count

Case 1: Rabbit activation

The following equation was used to calculate the activity of a radionuclide in the case when the sample was activated in the pneumatic transfer facility[15]:

$$\text{Activity} = \frac{N\,[e^{\lambda_x(CT-LT)} - 1]}{[1 - e^{-\lambda_x(LT)}][CT-LT]}$$

$$= \frac{N\,[e^{\lambda_X \Delta T} - 1]}{[1 - e^{-\lambda_X (LT)}]\,[\Delta T]} \qquad \text{(B-2)}$$

where

N = counts per second

λ_X = decay constant of the radionuclide

CT = counting time

LT = live time

ΔT = CT-LT = dead time of the detector

Case 2: Lazy Susan activation

The following equation was used to calculate the activity when the samples were irradiated in the Lazy Susan:

$$\text{Activity} = \frac{\lambda N}{[1 - e^{-\lambda (LT)}]} \qquad \text{(B-3)}$$

since for along activation where CT $\approx$ LT, equation (B-2) reduces to equation (B-3).

APPENDIX C

LINEAR COEFFICIENT CORRELATION

The linear coefficient correlation for the elements analyzed in the zircon samples:

	Ti	Al	Ca	V	Mn	Na	Dy	Fe	Co
Ti	1.0000	-.1580	.3697	.9738	.2863	-.0206	-.8671	.8163	-.1016
Al	-.1580	1.0000	.5695	-.0242	.5176	.4934	.3164	.4834	.9237
Ca	.3697	.5695	1.0000	.4690	.8723	.4374	.0422	.8782	.9312
V	.9738	-.0242	.4690	1.0000	.3362	-.0395	-.7849	.8537	-.1834
Mn	.2863	.5176	.8723	.3362	1.0000	.5305	-.1471	.5985	.9972
Na	-.0206	.4934	.4374	-.0395	.5305	1.0000	.0748	-.2975	.7724
Dy	-.8671	.3164	.0422	-.7849	-.1471	.0748	1.0000	-.6830	.1347
Fe	.8163	.4834	.8782	.8537	.5985	-.2975	-.6830	1.0000	-.1579
Co	-.1016	.9237	.9312	-.1834	.9972	.7724	.1347	-.1579	1.0000
Ba	.5163	-.1454	.6987	.4973	.6899	-.3117	-.3985	.7043	.3999
La	-.8279	.1152	-.5247	-.8266	-.2803	-.1737	.7987	-.7350	.2757
Sm	-.7772	.1878	-.4752	-.6727	-.3396	-.2904	.8254	-.4056	.1833
Yb	-.7461	.0375	-.5445	-.6382	-.4120	-.4135	.7654	-.3724	.0054
Lu	-.9485	-.0147	-.6421	-.9555	-.4618	-.1663	.9233	-.7922	.0912
U	-.9349	.0040	-.6477	-.9325	-.4904	-.1936	.9388	-.7848	-.0480
Sc	-.2517	-.4412	-.1776	-.3794	.0041	-.1534	.1090	-.0096	.4866
Cr	.7075	-.3997	-.2630	.6553	-.2142	-.4631	-.7361	.1667	-.5025
Zn	.4168	-.8156	-.5105	.2652	-.1701	-.2378	-.2739	.0000	.0000
Se	.4237	-.4102	-.5610	.5127	-.8291	-.5013	-.2718	1.0000	-1.0000
Ce	.4665	.0792	.7285	.5440	.6813	-.1871	-.2354	.8917	.5606
Eu	-.0172	.7661	.8157	.1213	.7096	.5063	.2798	.5312	.4591
Tb	-.3687	.6802	.4994	-.2513	.2567	.4052	.6570	-.3976	.6582
Zr	-.9111	-.1753	-.6513	-.9497	-.5376	-.1178	.7166	-.8884	.2383
Hf	-.9084	-.0975	-.5902	-.9326	-.4966	-.0400	.7479	-.8803	.3191
Th	-.5238	.0699	-.0314	-.5190	-.0367	.5829	.5373	-.5883	.4765

	Ba	La	Sm	Yb	Lu	U	Sc	Cr	Zn	Se
Ba	1.0000	-.2115	-.3694	-.4264	-.3559	-.4211	.3749	.2632	.5562	-1.0000
La	-.2115	1.0000	.9375	.9120	.9131	.9159	.3746	-.3892	-.8021	-.7592
Sm	-.3694	.9375	1.0000	.9625	.9519	.9644	.0786	-.4242	-.6377	-.4838
Yb	-.4264	.9120	.9625	1.0000	.9956	.9923	.0223	-.3096	-.1456	-.4933
Lu	-.3559	.9131	.9519	.9956	1.0000	.9915	.4253	-.5543	-.0638	-.5339
U	-.4211	.9159	.9644	.9923	.9915	1.0000	.3612	-.5814	-.2062	-.3968
Sc	.3749	.3746	.0786	.0223	.4253	.3612	1.0000	-.2774	.7100	-.8652
Cr	.2632	-.3892	-.4242	-.3096	-.5543	-.5814	-.2774	1.0000	.2348	-.0110
Zn	.5562	-.8021	-.6377	-.1456	-.0638	-.2062	.7100	.2348	1.0000	.1953
Se	-1.0000	-.7592	-.4838	-.4933	-.5339	-.3968	-.8652	-.0110	.1953	1.0000
Ce	.6492	-.3961	-.2520	-.2768	-.4926	-.4752	.2155	-.1057	-.9087	-.3758
Eu	.2584	-.1230	.1845	.0735	-.1859	-.2043	-.2417	-.3631	-.8493	-.7688
Tb	.0299	.3627	.5813	.4578	.4106	.4265	-.2664	-.5185	-.4108	-.4104
Zr	-.4783	.8205	.7484	.7374	.9636	.9365	.4057	-.4701	.2032	-.5754
Hf	-.4705	.7771	.7762	.7519	.9372	.9103	.3615	-.5033	.1742	-.5334
Th	-.5666	.7505	.7424	.7308	.8697	.8897	-.0059	-.5112	-.0014	-.1037

	Ce	Eu	Tb	Zr	Hf	Th
Ce	1.0000	.3743	-.1632	-.6503	-.6441	-.3123
Eu	.3743	1.0000	.6734	-.2885	-.1923	.1266
Tb	-.1632	.6734	1.0000	.1830	.3071	.2616
Zr	-.6503	-.2885	.1830	1.0000	.9861	.4622
Hf	-.6441	-.1923	.3071	.9861	1.0000	.4802
Th	-.3123	.1266	.2616	.4622	.4802	1.0000